Vegetation monitoring in coastal areas using readily available Remote Sensing data

H.S. Kathmann

Technische Universiteit Delft

Vegetation monitoring in coastal areas using readily available Remote Sensing data

by

H.S. Kathmann

to obtain the degree of Master of Science
in Applied Earth Sciences (Geoscience and Remote Sensing)
at the Delft University of Technology,

Student number:	5185955	
Project duration:	May 1, 2021 – April 20, 2022	
Supervisor:	Dr. R. C. Lindenbergh,	TU Delft, supervisor
Thesis committee:	Ir. A.L. van Natijne ,	TU Delft
	Dr. ir. S. de Vries,	TU Delft

Delft University of Technology

Abstract

Monitoring the status of the vegetation is required for nature conservation. This monitoring task is time consuming as kilometers of area have to be investigated and classified. To make this task more manageable, remote sensing has been included in the information used for this process. This remote sensing data is mostly used in the form of aerial imagery taken from airplanes.

The acquisition of airplane remote sensing data is dependent on weather conditions and permission to fly in airspace above the Netherlands. These conditions make it difficult to find a suitable time, resulting in not being able to get an new image every year. This procedure costs also money as the airplane has to be on stand-by until the conditions are actually met. For this reason alternatives for this dependency on dedicated airplane data is needed.

One of these alternatives is the use of optical satellite imagery, as this type of data has been improved rapidly in the last decade. As this data is now readily available, it can be used to create vegetation assessment on meter scales for multiple moments in the year. To improve the quality of the assessment the data is combined with other data sources. For this study satellite imagery from the Superview satellite is combined with geometric height data from the airborne laser scan dataset AHN.

The existing classification methods are not set-up for this amount of data to be combined. Therefore, a new method is required. In this study three different classification methods were prepared and compared. These methods are nearest centroid, random forest and neural network, from relatively simple too more involved. All these methods are able to do a supervised classification and output a probability for fuzzy classification. These methods were tested on 11 epochs on the Natura2000 dunal area Meijendel en Berkheide on the Dutch coast.

Our comparison shows that nearest centroid performs worse of the three models. The random forest and neural network perform similarly, for pure classes. But the transitions are better represented by the random forest method. This method has then be used to produce timelines to inspect vegetation transitions and other trends in the area.

The study show that the methods are suitable for detecting large scale vegetation processes, but validation of transitions is difficult due to the lack of training and validation data for these transitions. Improving by gathering in-situ training data could make this an viable way of supplementing the needed alternative for monitoring vegetation.

Contents

1 Introduction **1**
1.1 Model problems . . . 1
1.2 Meijendel & Berkheide . . . 3
1.3 Research questions . . . 3
1.4 Thesis structure . . . 4

2 Background information **5**
2.1 Dunes monitoring . . . 5
2.1.1 Dune systems . . . 5
2.1.2 Active processes in coastal dunes . . . 7
2.2 Remote sensing . . . 7
2.2.1 Resolution . . . 8
2.3 Optical imagery . . . 9
2.3.1 Airplane. . . . 9
2.3.2 Satellite . . . 9
2.4 LiDAR . . . 10
2.4.1 AHN . . . 11
2.5 Classification methods . . . 11
2.5.1 Original model: DICRANUM . . . 12
2.6 Data combination . . . 13

3 Area and Data **15**
3.1 Meijendel & Berkheide area . . . 15
3.2 Data overview . . . 15
3.2.1 Footprint . . . 16
3.3 Optical data . . . 16
3.3.1 Aerial photos. . . . 17
3.3.2 Satellite . . . 17
3.3.3 Superview satellite data . . . 17
3.4 AHN Height data . . . 18
3.5 Training . . . 18
3.6 Masking . . . 20
3.7 Conclusion Data . . . 20

4 Methodology **21**
4.1 Workflow . . . 21
4.2 Inputs . . . 21
4.3 Data alignment . . . 21
4.4 Training data generation . . . 22
4.5 Classification models . . . 23
4.5.1 Nearest centroid . . . 23
4.5.2 Random Forest . . . 24
4.5.3 Neural Network . . . 25

4.6 Classification products . . . 26
4.6.1 Classified Maps . . . 26
4.6.2 Probability . . . 27
4.6.3 Timeline generation. . . . 27
4.7 Accuracy assessment. . . . 27
4.8 Conclusion methodology . . . 27

5 Results 29
5.1 Introduction . . . 29
5.2 Classification . . . 29
5.2.1 Nearest Centroid . . . 29
5.2.2 Random forest. . . . 32
5.2.3 Neural Network . . . 34
5.3 Fuzzy classification . . . 36
5.4 Timeline of classes . . . 36
5.5 Case studies . . . 37
5.5.1 Transition to grass . . . 37
5.5.2 Transition to sand . . . 37
5.5.3 Redevelopment of dunes . . . 37
5.6 Conclusion Results . . . 41

6 Discussion 43
6.1 Data Quality . . . 43
6.2 Data processing . . . 44
6.3 Computational challenges . . . 44
6.4 Training . . . 45
6.4.1 Alternative Training sets . . . 45
6.5 Examination of model results . . . 45
6.5.1 Continuity of classification . . . 46
6.5.2 Probability to new class . . . 46

7 Conclusions and recommendations 47
7.1 Conclusions . . . 47
7.2 Recommendations. . . . 48

Bibliography 49

A Additional results 53

B ISPRS Paper 57

1
Introduction

Situation

Nature is a vital and integral part of our environment. It has many functions that are important to keep area's sustainable. One of these functions is to keep flora and fauna sustainable and healthy, by maintaining areas suitable for water storage and production of clean air. These nature-rich areas are protected to keep them available in an increasing urbanizing world. In Europe, nature reserves are protected under the Natura2000 program (Sundseth, 2008). The goal of this program is the protection of certain habitats. In every area, goals are set for every habitat type, these include the quality of the habitat type and their extent.

Reporting of the status of these habitats is required by Natura2000 to track the progress towards goals and where action should be taken. However, most of these nature reserves are quite large, which makes it difficult to monitor them from the ground. This problem can be solved by seeing the area from a whole other point of view, by using remote sensing data these kilometer large areas can be analysed efficiently.

Remote sensing is the process of acquiring data from a distance (Cracknell, 2007), in this context it is the acquirement of physical information of the coastal area. Not all forms of remote sensing data are the same, the detail needed for monitoring on this scale used to be acquired by airplanes (Kasampalis et al., 2018). These planes have limitations on when they can fly, when allowed by airspace control and when the weather is good enough. Also this practice is costly as planes have to be on standby to fly-out. However there are now viable alternatives for data as acquired by planes. For example satellite data is becoming more viable for detailed classification (Leimgruber et al., 2005), with better spatial resolution to track more detailed changes. They don't need permission to fly, and will have new data points available more often. However, this also means that sometimes these points will be obtained during unfavourable weather conditions, like on cloudy days.

1.1 Model problems

To decrease the workload of the monitoring, classification can be partly automatized using computer modelling. Classification models are typically not generic, most models work best with only one type of airborne data. As more types of data are available, these additional data types should be used in this model. A model might be able to work with optical satellite data. However, it will still be limited as only a limited portion of the data can be used. Other more modern classification methods may provide better results as they include more types of input

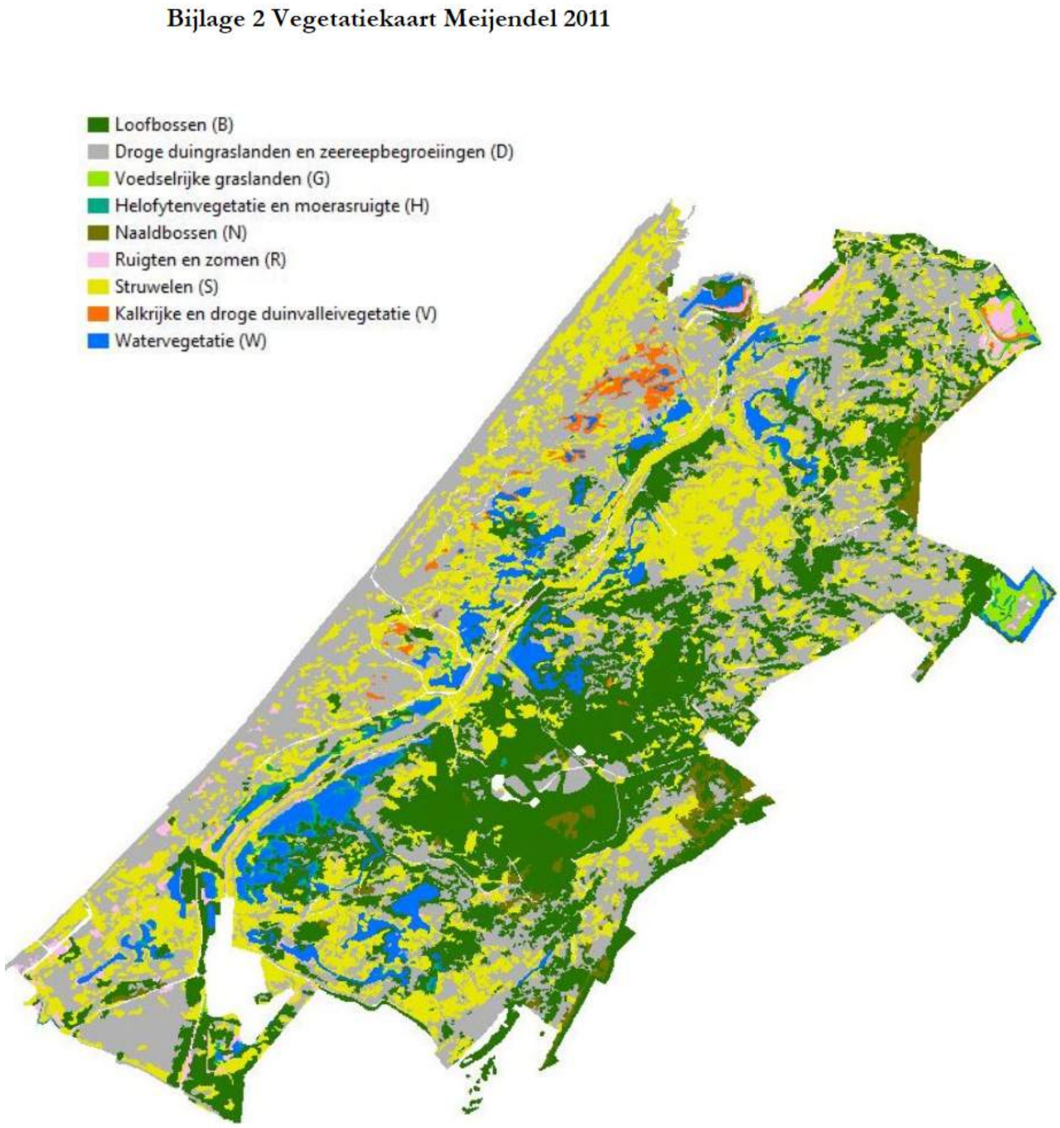

Figure 1.1: Example of an vegetation map for the Meijendel area, showing the structure of vegetation and the scale that is required (from Janssen et al., 2015)

Figure 1.2: Image taken in Meijendel on 27th October 2021, typical dunal landscape for the area, important habitat for the area

data (Abburu and Babu Golla, 2015).

The underlying method of models has improved with the increased availability of computational power available, these more sophisticated classification can take advantage of more data, both input data and training points. Newer model types can use more data simultaneously resulting in overall better models. However, more data might mean more training data needed and longer computational time. The combination of data types can boost results (Schmitt and Zhu, 2016). The improvements gained from newer types of classifications, should be compared to the drawbacks that result from this.

In this study new models for classification of vegetation will be explored and compared. These models will make use a combination of satellite and geometric information. These data sources can be seen as an alternative to the exiting methods that use only airplane imagery. This will show the feasibility of including new data types and the advantage of data combination.

1.2 Meijendel & Berkheide

The area where the classification methods were tested is the Meijendel & Berkheide area in the Netherlands. This area along the dutch coast is a Natura2000 nature reserve. This will mean that monitoring is an vital part for the nature preservation in the area. The area consists of a varied and extensive dune landscape, and is relatively rich in relief.

The area is split into the two separate areas: the southern Meijendel area with extensive dune plains, and the northern Berkheide which consists of dunes on top of the original riverbed of the old Rhine. These calcareous-rich dune grasslands are characteristic for this area, an example of this dunal landscape is shown in figure 1.2.

1.3 Research questions

The main research question is *How can readily available remote sensing data give reliable and up-to-date vegetation classification in coastal dunes?*

1. What are the desired properties of the end-product?
The end product is an important factor as it determines the scale at which the processing should be focused, it should also be clear what the end-product should include to give enough information while still being easily readable and understandable. Another factor that should be how often new data should be reported.

2. What suitable satellite and aerial data is readily available for the selected area, time period and application?
There are lots of sources of data, with all kinds of data types and temporal resolutions. From all these source the most suitable data sets should be identified. This selection should explore the sources on the strong and weak points of each of the data sources, for example the availability and the data size.

3. How is data currently processed for obtaining vegetation maps?
An exploration of previous methods of data processes can give ideas how to efficiently process all kinds of data and how vegetation is now monitored.

4. What natural processes can be determined by each data type?
The coastal dune area will have a lot of processes that can cause changes in the landscape, each of these processes will have a different time scale and spatial effect. In this part several processes will be investigated and the data sources will be checked on if they can recognize the effect of the processes, and which data set might can best recognize each natural process.

5. How can data from different sources be processed?
The data sources all have different data types, therefore they have to be standardized so they can be compared and combined. Some data sources will have differing units that have to be compared and standardized units to not overemphasise any data source.

6. How can the quality of the final product be determined?
If we would like to compare results, a metric should be made by which each result can be compared. A quality score should be some form of accuracy and might be checked against the actual real-world situation. What quality would be enough for the end product to be considered valid and usable product.

1.4 Thesis structure

Chapter 2 starts with background information about monitoring and remote sensing basics. Chapter 3 of the thesis is be an introduction into the data we intend to use for the classification, and an introduction to the area of interest. Chapter 4 discusses classification methods we intent to investigate starting with the model that is now in use, and getting more complicated with every step. Chapter 5 the resulting classifications are compared, and the strong and weak points of every classification are shown. Chapter 6 discusses on what assumptions have been made and where potential errors may arise and then in Chapter 7 concludes with an overview of the models and the usability of the results, a recommendation for the best model to use and a recommendations for further research and developments.

2

Background information

In this chapter the need for monitoring and what the requirements of the monitoring are, are explained. A part about how this monitoring is done now using existing models, and how these models work. Then a section on the types of remote sensing data that are available.

2.1 Dunes monitoring

Monitoring is the process of assessing the status of certain processes and the quality of the monitored objects over time. In this case the monitoring of vegetation is a way to assess to processes going on in nature, and then to see if action is needed to protect the vegetation type (van Beek et al., 2018).

The task of monitoring used to be an very labour intensive task, it would mean that someone had to go through every spot in the whole area that had to be monitored and record in some way the state of the vegetation. This time-intensive task would mean that for large areas the whole monitoring job could take years to complete. Now it has been made easier by first selecting areas which look like they belong to the same type based on aerial images. Furthermore, comparing of older imagery can show long-term trends that are difficult to observe from the ground (Lasanta and Vicente-Serrano, 2012).

For a Natura2000 area the trends of habitats in these area's have to be reported every 6 years. Where for each area certain habitats are assigned to be characteristic for each area (Sundseth, 2008). These habitat types get targets if they should be expanded or maintained. Also the quality of each habitats is considered and targets are set if the quality of these habitats should be improved.

2.1.1 Dune systems

Coastal dunes are an important habitat created by combinations of wind and water's effect on sand particles. All over the world dune systems can be found, see Figure 2.1, for this project we only focus on coastal dunes.

Within the dune systems there are different types of habitats, within the area of interest the more sand-types of habitats are white dunes, grey dunes, shrublands, dune forests and wet dune valleys. Whereas some more vegetated types exist as dune shrubs and dune forests.

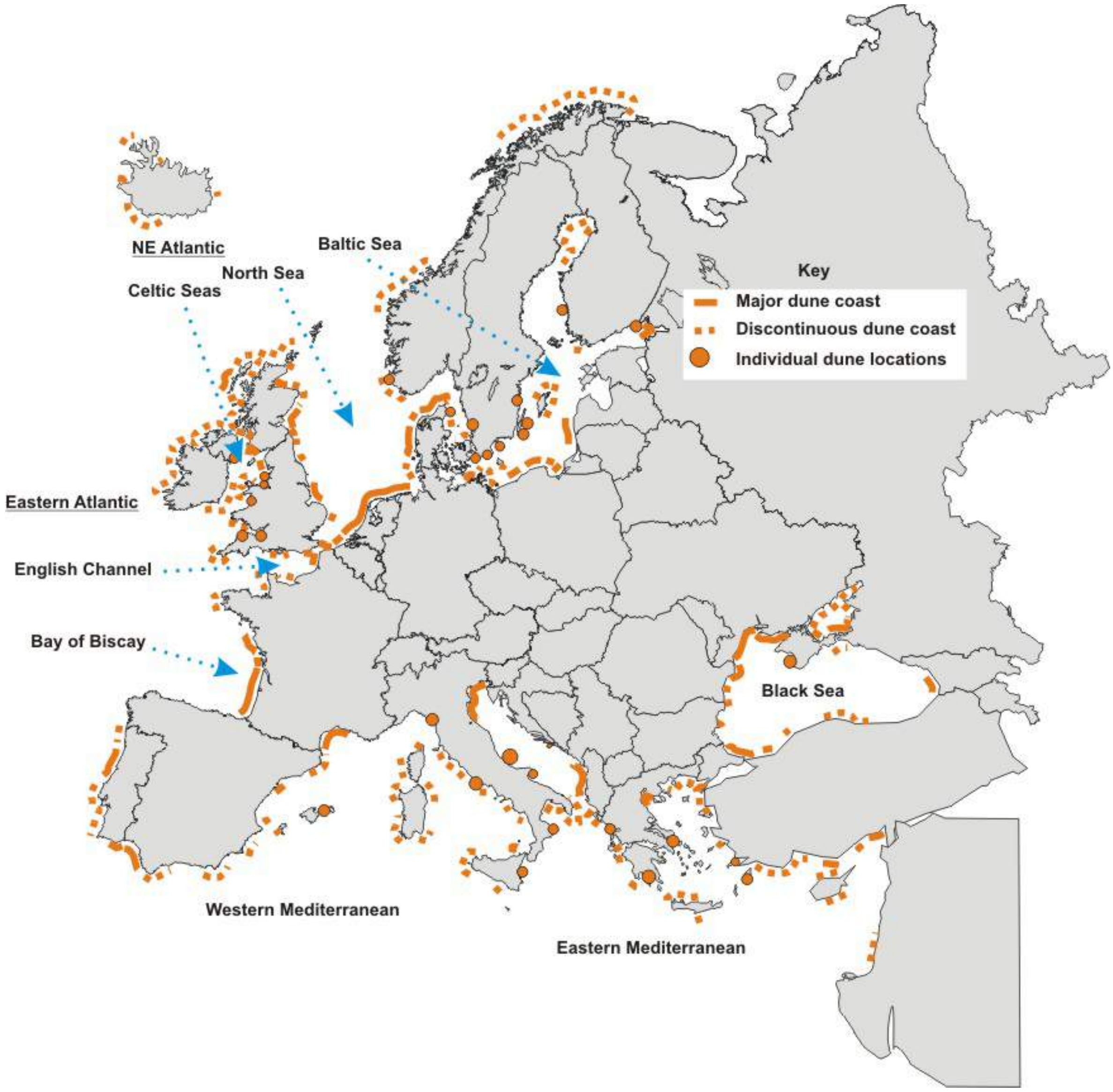

Figure 2.1: Coastal dune distribution around Europe (from Doody (2012))

Dune types

The first type is white dunes (Natura2000 code H2120) (Ministerie van Landbouw, Natuur en Voedselkwaliteit, 2005), these are relatively new dunes that mostly found close to the coast. These dunes are called white dunes because no soil forming has happened that will turn the sand to a greyish color. For these dunes to stay the same quality sand has to be transported around, this dynamic status is mostly caused by wind transported sand. The vegetation in this habitat is mostly in the form of marram grass as this is one of the only vegetation types that can survive in this dynamic landscape.

The next habitat is the grey dunes (H2130), this is one of the most extensive habitat types in the Meijendel & Berkheide area. This habitat type is made of sand with less wind dynamic, this means that vegetation is more likely to grow here. In the habitat types this habitat has two forms calcium-rich and low in calcium. The quality of this habitat can be maintained by keeping the vegetation short (less than 50cm height) and thin. This could be done by grazing of animals to keep the vegetation manageable, naturally this is be done by keeping rabbit populations.

The shrubland habitat (H2160) are characterized by the domination of several types of shrubs. Most often in the form of the sea bucktorn, which grow well on white dunes. This habitat grows on ground that is also suitable for white to grey dunes, an health balance between more shrubs or more grey dunes is the goal. The rise of shrubland growth is related to an decline of rabbit populations.

Dune forests (H2180) exists of decidious forest, partly natural and another part man-made. The most common tree species is the oak, however, other tree species can also be found in this habitat. Coniferous trees are not part of this habitat but are able to be redeveloped to this habitat type. There are three subtypes of the habitat; the dry, wet and inner dune edge.

Humid dune-valleys (H2190) are wet areas, ranging from open water, wet grassland, with low swamp vegetation till reed land. And all the transitions between these areas. These areas mostly exist at areas where the dunes valleys are blown out to under the groundwater level. These areas can change over time, in dry periods the water can almost totally disappear from these areas. However in wet times the areas can also grow out of the original area.

2.1.2 Active processes in coastal dunes

In the dunes there are several active processes, that occur naturally mostly by the influence of sea and wind. If the wind does not keep the sand moving, vegetation will start to grow between the sand. Some area's have not enough vegetation which results in empty dunes which are prone to damage by wind. However, totally overgrown dunes are not preferred either, too much vegetation disrupts the natural dynamics of the coastal landscape. This characteristic landscape is what the Natura2000 tries to protect.

2.2 Remote sensing

Remote sensing is the technique of getting information about a target without making any contact with the target. There are two types of remote sensing, passive remote sensing only measures the radiation from the object. This can be in emitted or reflected radiation, most of this reflected light is reflected sunlight. The other form is active remote sensing, here a signal is send from the satellite and the reflection of this signal is being recorded. Examples of this type of remote sensing are LiDAR and Radar (Rees, 2013).

The standard form of passive remote sensing are airborne photos. In this basic form these photos only record the reflectance from the ground being recorded in a spectrum between

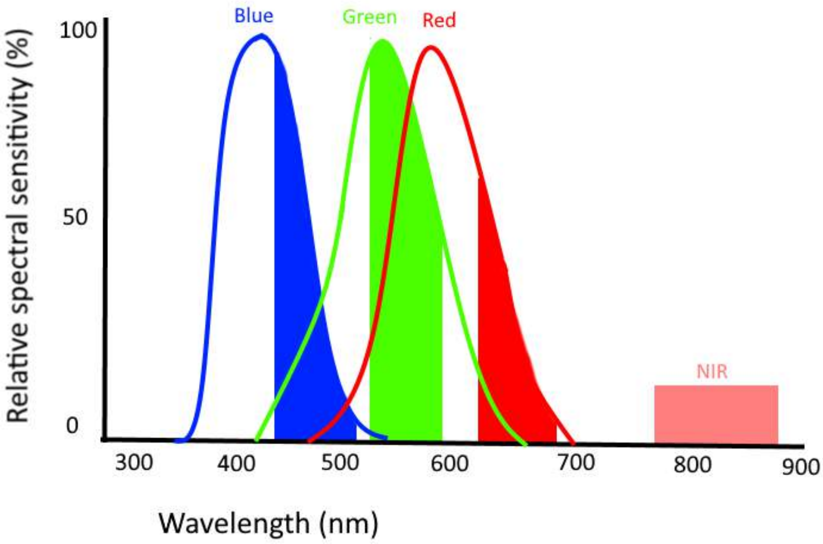

Figure 2.2: Electromagnetic spectrum to RGBI bands, the curves are the sensitivity of the photo receptors in our eyes, colored-in boxes show the sensitivity range of superviews sensor for each band.

black and white. However this greyscale imagery has long been replace by color imagery, This is done by separating measurements in only specific parts of the electromagnetic spectrum. These selective ranges we perceive as certain colors. The colors that are most often chosen for this purpose are the primary colors of red, green and blue. These colors range can for example be 630-690nm for red, 520-590nm for green and 450-520nm for blue in the electromagnetic spectrum as can be seen in Figure 2.2. The Near infra-red is outside of the visual range for our eyes, often in the range of 750-900nm.

Images of color are good for visualization purposes, but most optical datasets have other bands that can give more information. An often included band is the band into the Near-Infrared (NIR). This information is beneficial for vegetation classification as the reflection is very dependable on chlorophyll as shown in De Boer (1993). Some optical data goes even further in the spectrum to thermal infrared, but these datasets are not as widely available.

2.2.1 Resolution

There are three different types of resolution that have to be considered in remote sensing. The first resolution is spatial resolution this is the size of a pixel on the ground, this has been improving in recent years. For satellites this used to be in the 10s of meter but has been getting into the sub-meter level.

Another resolution is the spectral resolution, this measure is the amount of spectral information that is being captured by the sensor. This can be quantified in the number of bands, with more bands having a bigger part of the spectrum.

The last resolution is the temporal resolution, is more related to the platform of the sensor. It gives the frequency that new data is collected, for example a new image every day or only once per year.

Figure 2.3: Example image of the Aerial imagery from airplane made available by Beeldmateriaal.nl, inset map futher zoomed-in version to show effective pixel size.

2.3 Optical imagery

2.3.1 Airplane

Aerial data is the most widely used form of remote sensing data, with images that have high spatial resolutions, see Figure 2.3, and have more bands with information. From greyscale to red, green and blue color bands and increasingly more often bands in the Near-Infrared. However the big drawback is that the Dutch airspace is busy and weather is quite often unfavourable for creating those high quality images. This results very few suitable moments for aerial imagery to be acquired and a lot of costly stand-by time for these airplane.

2.3.2 Satellite

Satellite remote sensing has been around since the 1970's. The launch of the LandSat program made this global remote sensing available to a broader audience. A lot more programs has been launched over the years, with higher spatial resolutions.

While the satellite imagery is often worse in the aspect of spatial resolution than airplane imagery, the main advantage of it is that satellites take images repeatedly, some even every day. While not all of these images will be usable, for example because of unfavourable weather conditions over the target area, it is a lot more cost effective than any other repeatable imagery.

The satellite data used for this report is mostly taken from the Superview platform. This Chinese platform has been launched in 2016, it operates in an orbit at 530km. From that height it takes images with a spatial resolution of 0.5 meters. These images are about 12 kilometer wide, this results in the ability to capture about 700.000 square kilometers per day (Spacewil-

Figure 2.4: Example image of the Superview satellite imagery, inset map zoomed version to show effective pixel size.

IInfo, 2020). Part of an superview image is shown in Figure 2.4

This data has been made readily available by the Netherlands Space Office (NSO (n.d.)), in their program the imagery is bought and made freely available about 5 to 6 times per year. Not all the imagery dates might be suitable for classification as clouds could have obstructed the view of the area of interest. The superview satellite sensor capture imagery in Red, Green, Blue and Near-infrared bands.

2.4 LiDAR

LiDAR or the name Light Detection And Ranging is a technique of using laser pulse to detect distances. This is done by emitting a short pulse of light towards an target and waiting for the reflected echo to be detected some time later. This delay together with the speed of light, is used to compute the distances (Rees, 2013).

$$D = \frac{c \cdot t}{2}$$

where:

D = range or distance,
c = speed of light, and
t = time between sending and receiving of pulse

This process is typically used to make height measurements, where the height of the surface

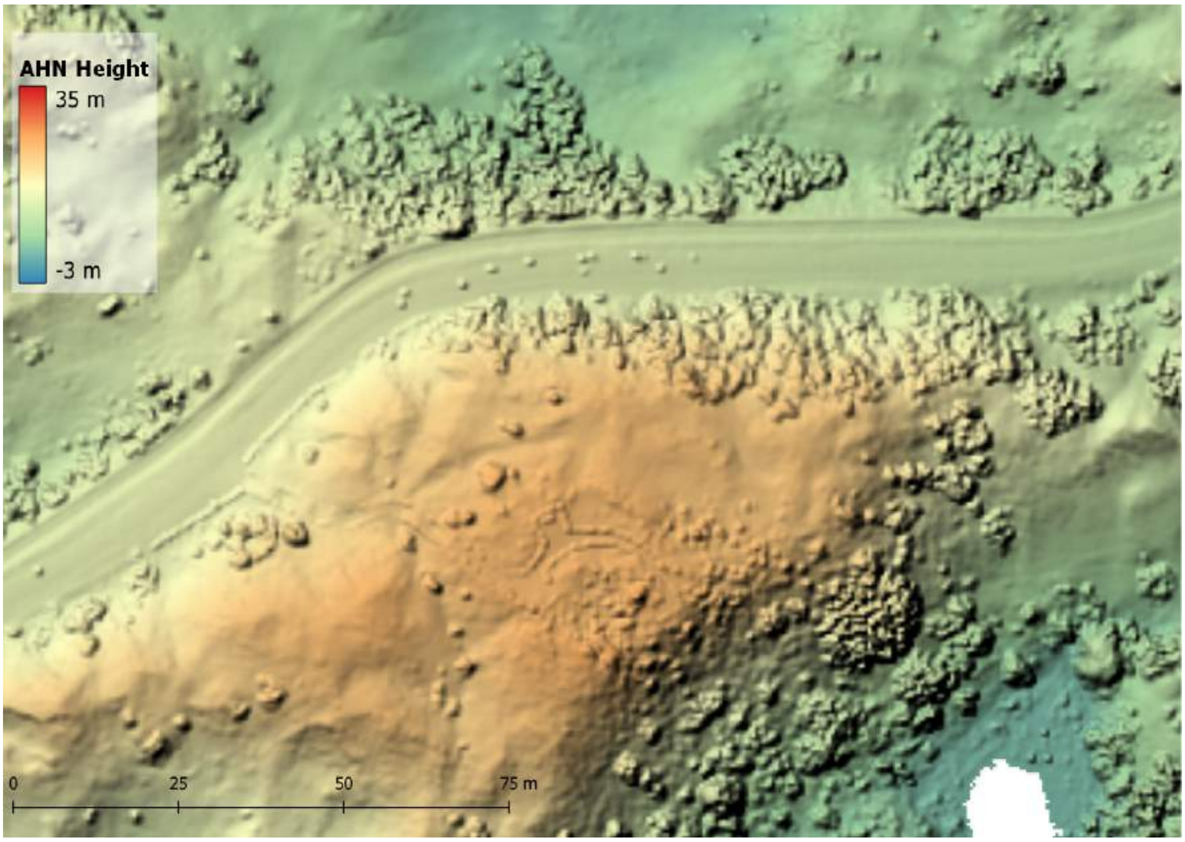

Figure 2.5: Example of AHN height raster dataset from same location as other example, taken from 0.5 meter raster file, The hole with no data at bottom left corner is water

can than be computed from the distance of the vehicle to the where the pulse reflected. One of the biggest strengths is that for every location multiple reflections can be distinguished, this can for example mean that for a tree the top of the canopy can be measured, while also receiving a slightly delayed reflection from the ground below that tree. All these reflections can be viewed in a LiDAR point cloud, where each point shows the location of a reflection in 3D space.

2.4.1 AHN

The most well-known LiDAR height datasets for the Netherlands is the AHN, the Actueel Hoogtebestand Nederland. This dataset has elevation data for the whole area of the Netherlands. This high quality dataset can be used in raw point cloud form or in the derived raster based datasets. These rasters are combined on scales of 0.5 and 5 meter squares, an example of this raster is shown in Figure 2.5.

This rasterized dataset is available in an version with values for the first return points, and a processed version where all the ground heights are estimated. This processed version is based on the last return points and some interpolation.

2.5 Classification methods

There are many different ways to classify the vegetation for large areas. They can be split in two different camps, pixel-based and object-based. Pixel-based methods classify each pixel separately, while the object-based variants first make groups of similar pixels and then give each group a certain classification (Abburu and Babu Golla, 2015).

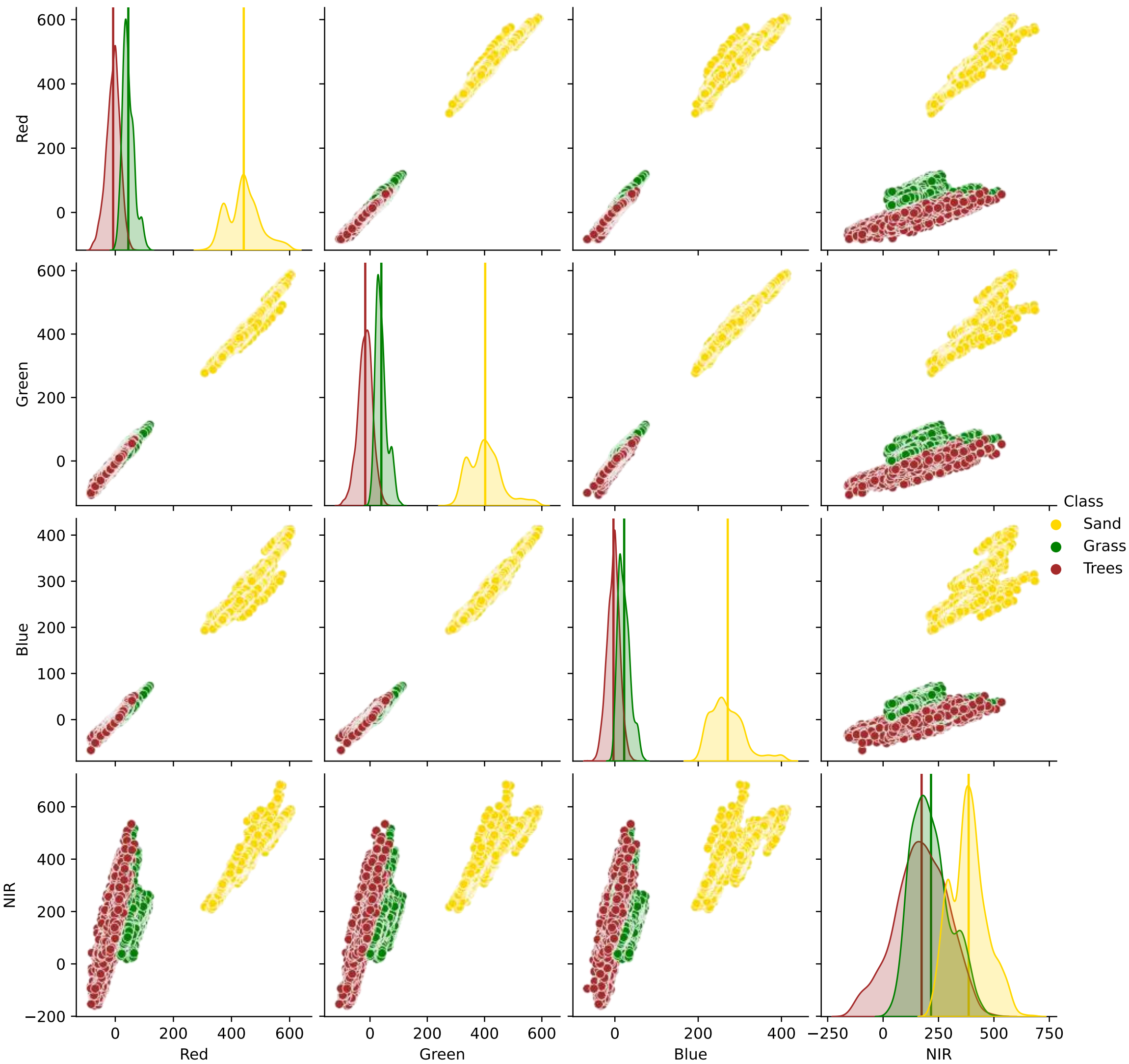

Figure 2.6: Example of feature space. Red, Green and Blue bands give very similar values. While the Near-infrared give other information causing better separation in feature space.

2.5.1 Original model: DICRANUM

To explore a model we take the example of the model that has been used at Meijendel before. This model is an extension called DICRANUM (Assendorp, 2010). As this is an older model the method behind it is simple by modern standards.

As input the model takes data from only the red and near-infrared spectral images, using these two bands the model is trained. These spectral bands are selected because the give they most information in the ratio between the bands to get the best results. In Figure 2.6 it can be seen that red, green and blue are all very correlated, getting separation between classes using these bands is difficult while the Near Infrared introduce more information for the class separation.

Using this the classes have to be defined, for this DICRANUM these classes fall on a spectrum of bare ground with no vegetation to a class with 100% coverage with shrubs and trees. Between these so called crisp classes, that are mostly homogeneous over several pixels. Additionally there are 5 fuzzy grassland classes which are in the sub-pixels level.

While a pixel can belong to a crisp class, the fuzzy classes can often be smaller than the whole pixel. These are therefore only the proportion of the pixel that likely belongs to the class is given. The so called membership value gives the probability that the pixel belongs in that fuzzy class. A pixel can have membership values belonging to several fuzzy classes. This fuzzy classification is well suited for vegetation monitoring as de Lange and van Til (2004) shows.

The crisp classes are described by using a process where samples belonging to the crisp class are selected on the image. The samples are put into the feature space of red-infrared reflection. If done correctly each class should be placed on separated parts of the feature space. Around these regions a polygon can be placed. The classification processes then only has to check if the spectral information of a pixel falls within one of the polygons to see if it can be classified into one of the crisp classes.

All pixels that do not fall into one of these polygons in the feature space will be classified by the next step, the construction of the fuzzy classes. For this step field observations are needed, where an expert will sample ground points placed using GPS. Where each sample contains the percentages of the fuzzy classes to which that point belongs. Using these field samples, the spectral information of these points can be extracted from the images and be put into the feature space. Using some interpolation method the member ship values of each of the fuzzy classes can be estimated in the feature space.

Application of the classification is straightforward. The only thing that has to be done is extracting the red and near-infrared value of each pixel. Looking in the feature space and extracting the crisp class or the membership values of the fuzzy class that the pixel belongs to. This can result in 6 maps, one with only the crisp classes shown and 5 with the membership values for each of the fuzzy classes. To get an actual final result, these can be merged into one map by showing the crisp class or the highest fuzzy class.

The strengths of this model are the ease use of the model, and the high accuracy of the crisp classes. However the disadvantages of the model are the limited data that can be used and the need for field observations to get the fuzzy classes.

2.6 Data combination

With the increase in data available and computational power that is able to work with more complex models, the input data is getting more elaborate. Example of this could be hyperspectral where a lot of different bands are used to get more spectral information, in for example Schmidt et al. (2004) this is used to automate classification.

Other combinations where the ratio of several bands proves more useful than the data from the bands alone, the most prominent example of this are vegetation indices like NDVI (Schmitt and Zhu, 2016; Bannari et al., 1995). But also the combination of imagery with geometric information like heights proves to be very useful, see Hantson et al. (2012) and Kempeneers et al. (2009).

3

Area and Data

This chapter introduces the area, and provides a description of the data that is used in the study. Class definitions and data pre-processing is described in the methodology.

3.1 Meijendel & Berkheide area

The area of interest consists of the Meijendel and Berkheide dunes (Figure 3.1). It is situated at the coast between the cities of The Hague and Katwijk. The area has a size of 2877 hectares, the southern part is called Meijendel and is the larger area at 1951 hectare while the northern Berkheide is 926 hectare. This combined area is officially defined as a Natura2000 area, with the Berkheide also being a protected nature reserve.

3.2 Data overview

The data used for this thesis should fulfill certain parameters: it should be up to date, easily accessible and ready to use. These points are summarized in the tables 3.1 and 3.2.

The data sets each have their own advantages, in the first table 3.1, the specifications of each dataset are described. The AHN has a raw form with point density, while the processed rasterized form is available in both 50cm and 5 meter grid versions. The satellite has the same type of bands as the aerial imagery available. Moreover other satellite data is available for dates before 2019. This data has a larger pixelsize making classification less detailed.

In the second table 3.2 comments are made about the datasets. The AHN has very precise height data, especially when used in the point form. However this processing is difficult with the other datasets which are always in raster form. The satellite imagery has lower resolution with better data availability compared to the aerial variant.

The final data after processing has to be at least on the sub-meter resolution, cover at least 80% of the area of interest and be in the RD-system. This RijksDriehoek coordinate system is

Name	Type	Resolution	Temporal	Availability
AHN	LIDAR	50cm/5m	Every 6 year	2008, 2014, 2021
Superview	RGBI	50cm	monthly	2019-now
Aerial photo	RGBI	25cm	yearly	2016-now

Table 3.1: Overview of readily available data considered in this study.

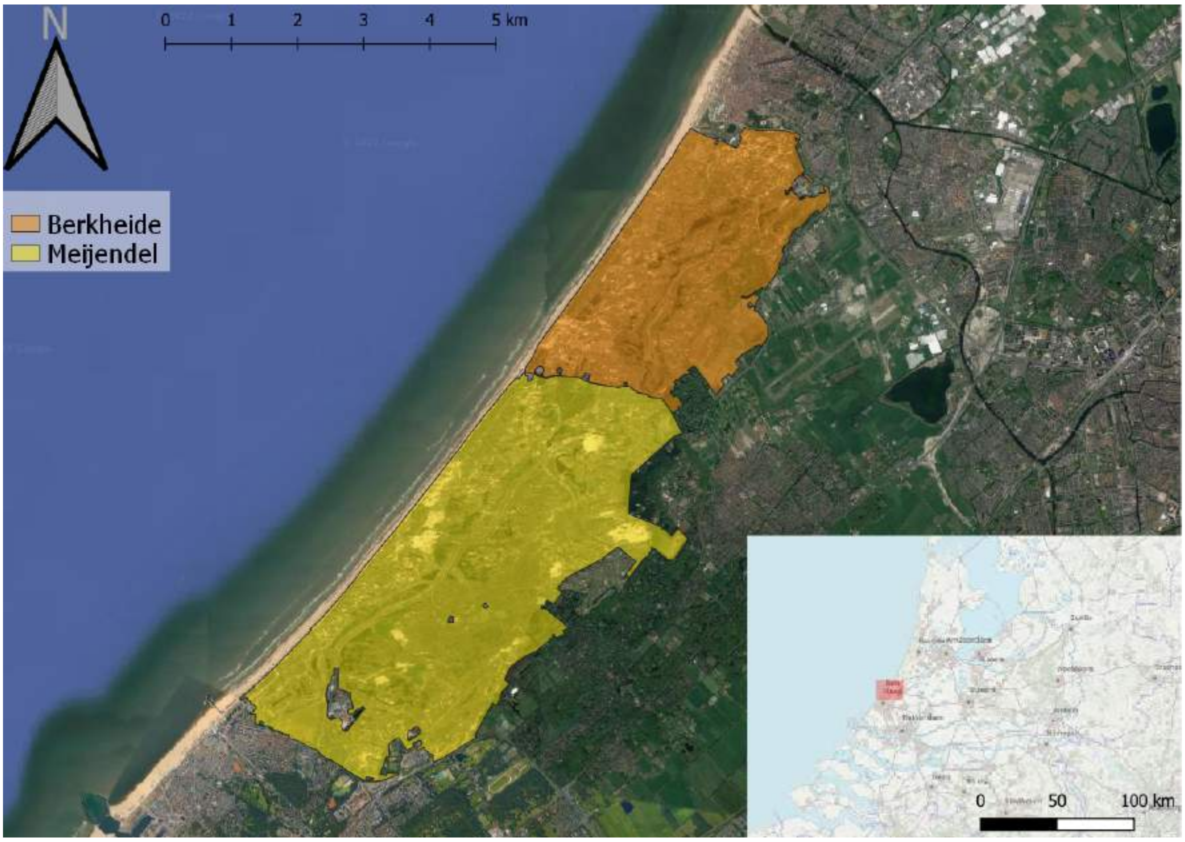

Figure 3.1: Study Area, Meijendel and Berkheide, Background Google satellite

Name	Strong Points	Weak points
AHN	High elevation accuracy	Large files
Superview	Monthly acquisition	Footprint not consistent
Aerial photo	Best resolution	Only yearly

Table 3.2: Summarized advantages and disadvantages of data sources

the standard coordinate system for Dutch geographical data. This makes the datasets easier to align and easier to implement into methods that already use other Dutch datasets.

3.2.1 Footprint

Each dataset has its own coverage and distribution methods. For example some datasets have been put into standardized footprint areas of 5 by 6.25 km, while most satellite imagery takes images along it orbit with sizes larger than 10 by 10 kilometers. The coverage of these satellite imagery footprints is not always the same, as Figure 3.2 shows.

3.3 Optical data

For the data there are several platforms to choose from. From them we want to use readily available data. This means that these datasets can be used without having to buy data directly from the source companies.

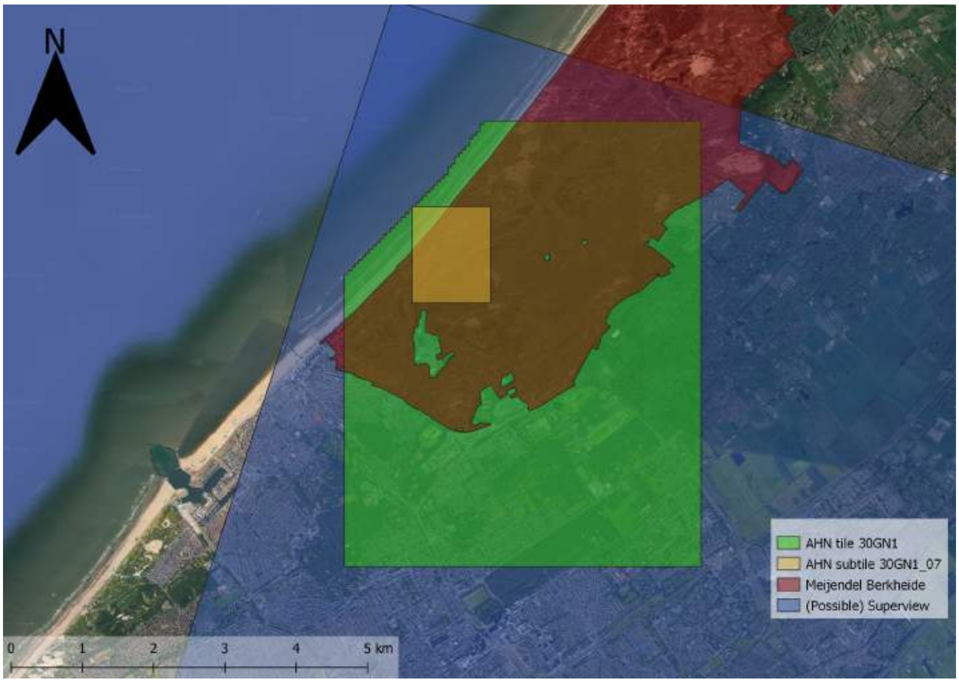

Figure 3.2: Footprints of data sources, Superview imagery have several footprints that include the area of interest. Background: Google Earth

3.3.1 Aerial photos

The aerial photos that are readily available in the Netherlands are made available by Beeldmateriaal.nl. This dataset contains imagery with a spatial resolution of 25cm, using the red, green and blue bands together with a Near-Infrared band. This dataset is available since 2016, however it is only created once per year. The dataset is captured somewhere between the 1st of April till half July, it is only flown when the weather is favourable.

3.3.2 Satellite

There are multiple open access satellite data sources. The LandSat program run by NASA is the longest running satellite data source, which has been freely available since 2008. This satellite program has a continuous dataset with new satellite launches giving the program access to better resolutions. However, the resolution of the newest satellite only reaches 15 meters, which is not suitable for this projects needs.

The European equivalent of the LandSat program, is the Sentinel program. The Sentinel 2, the optical satellite mission of the program, was first launched in 2015. This satellite produces slightly higher resolutions at 10 meter, which is still too coarse for the type of vegetation assessment in the study.

3.3.3 Superview satellite data

The satellite data is taken from the Superview platform, about 5 times a year a new image is bought by the Netherlands Space Office and made available for use by Dutch entities. As this dataset is bought for whole swaths of the Netherlands, not all data points are over the area of interest or of suitable quality. In Table 3.3 the Superview images that are available are shown with a short comment and if they are being used in our case study.

Dates	Used	Comments
2019-03-02		Fluffy cloud cover
2019-04-01		Only western edge of area
2019-04-22	x	Earliest usable Superview image, missing South-West corner
2019-06-01	x	Full image, dry period
2019-07-21	x	Full image
2019-09-18		Cloud cover over western part
2020-03-11	x	Slight haze over southern part
2020-05-08	x	Full image
2020-06-25	x	Missing South-West corner
2020-09-15	x	Full image
2020-12-31		Cloud shadows over southern area
2021-03-02	x	Full image, low tree cover
2021-04-23	x	Full image
2021-06-03		Total cloud cover
2021-09-07	x	Full image
2021-10-09	x	Missing Northern East corner

Table 3.3: Superview data availability, as acquired from NSO SatellietDataportaal, comments are based on visual inspection

3.4 AHN Height data

The height data that is being used to estimate the vegetation height comes from the Actueel Hoogtebestand Nederland dataset (AHN, n.d.). New versions of this dataset take years to produce, therefore a new version is only made every $\tilde{6}$ years. The most recent version (AHN4) has been produced in 2020 and the first data was made available in 2021. The version before this, AHN3, was produced between 2014 and 2019. To improve the chance that the height data has the same underlying information as the optical data shows, only the recent AHN4 data has been used for the model.

The vegetation height is estimated by taking the raster images with a pixel size of 0.5 meters. The DTM and DSM are two different products that are produced from the AHN lidar data. By using both these the difference between the ground and surface at the top of vegetation can be found. This step only has to be done once to get an estimated vegetation height grid for the whole area.

3.5 Training

To classify the area the classes should be defined, both in what belong to each class but also how this data is being saved to be put into each model. The way the training data is being collected can be have a great effect on the results of the classification. Therefore this reason the training method has to be standardized to create the most accurate comparison.

The classes are mostly based on the vegetation state of coastal areas. The first class is therefore sand, an important part of the dunal area. The next class is the grass class, with low dune grass and some moss. Then the last class is the bigger vegetation, for example trees and bigger bushes are part of this class. Visual examples of these classes are shown in figure 3.3, also with examples how these classes look in the field.

(a) Sand from satellite

(b) Sand in the field

(c) Grass from satellite

(d) Grass in the field

(e) Trees from satellite imagery

(f) Trees in the field

Figure 3.3: Examples of classes. Left column: Superview data of 07 September 2021. Right column: field photos, made in Meijendel by author

Classes	Description
Sand	Class consisting of sand mainly in the dunes
Grass	Grass and bare ground, with some dune grasses as vegetation
Trees	Any vegetation higher than a 2 meters till big trees of several meters high

Table 3.4: Description of the training classes used for the classification models.

3.6 Masking

As the classifier method is tuned to classify vegetation, non vegetatation is filtered out. To achieve this water and buildings are masked, Furthermore roads and parking lots have to be filtered out to block out the asphalt. For this several vector layers have been combined, first of all the BasisRegisratie Topografie (BRT) has been used for road (wegdeel) and buildings (gebouw). Then the watermask is extracted from the BRT (waterdeel) Then the last mask is hiding all the area outside of the area of interest including the sea. All these areas are combined into a single mask that can be put over all the results, to only show the relevant area of interest.

3.7 Conclusion Data

The data considered for this study are all forms of remote sensing data. The data should be ready to use and relatively up to date. For these reasons the dataset for optical data is from the Superview satellite, this data source has imagery in the red, green, blue and Near-infrared bands. For the geometric data the AHN data is being used, the addition of this dataset adds another dimension to the classification.

The classification needs definition of the classes. The three classes; sand, grass and trees are described. For each of these classes examples have to be located for the model to be trained on. These training areas can then be put into the methods described in the next chapter.

4 Methodology

This chapter presents our methodology to apply on the readily available data, introduced in Chapter 3, to obtain a vegetation classification map. Firest the workflow is expalined where every step is explained further in the chapter. From preparing data, to classification models and then accuracy assessment. Then the model selection is explained, including how each model works and what parameters can be set. Last, what the output data will produce and how this can be visualized for further use.

4.1 Workflow

The workflow is separated into three separate parts as can be seen in Figure 4.1: the data input and data alignment, the training and predicting of the model and then using the output to generate output maps and timelines. The input data has been described in Chapter 3, this will be equal for every model as to not give bias to any models strengths. Then this data is processed by each of the three models, for each of these models the training input data is the same.

4.2 Inputs

The data that we use for the models is explained in Chapter 3, the optical satellite data from the Superview satellite. Containing a red, green, blue and Near-infrared band. And two datasets produced from AHN elevation data, a surface model with the highest points and a terrain model with the ground elevation.

4.3 Data alignment

The first thing that has to be done is pre-process the data so that it will be efficiently put into the models. To do this all the datasets have to be aligned to the same specifications. This includes the requirements that all the datasets fill the whole area of interest, use the same spatial resolution and are aligned in the same coordinate system (Yehia et al., 2019).

The area that is covered by each dataset varies and most have (large) areas of data outside the area of interest (Figure 3.2). This unneeded data will cost storage space and cause longer processing time. Therefore, all data will first be clipped to the bounding box around the area of interest, then it will be re-projected to a grid in the RD system with a ground pixel size of 1 meter. Not every data layers will totally fill this area, a dataset that fills less than 75% of the area with valid data will be ignored from further processing. These invalid pixels could

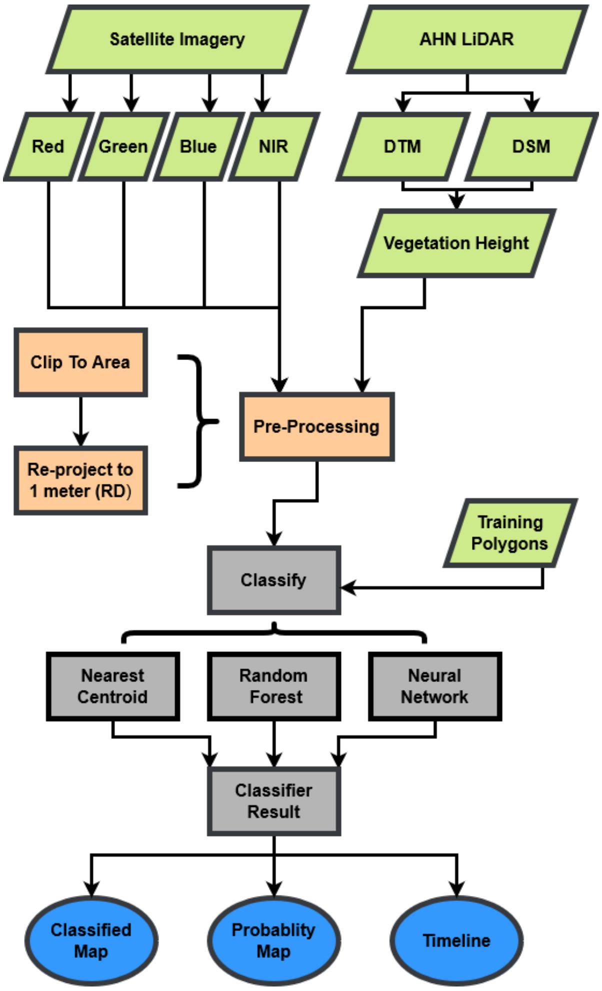

Figure 4.1: Workflow of processes, Seperated in four stages, Input (green) -> data alignment (orange) -> Classification (grey) -> Final products (blue).

be caused by satellite images that are cut off in the middle of the area, or by too much cloud cover.

4.4 Training data generation

Before the classification can be done the training data has to be made. It would be very time consuming to make a new training dataset for every date, this could also introduce bias based on the quality of the training points. Every date will use the same training points, these points are areas of 10 by 10 meters which have only a single class as can be seen in Figure 4.2. By including an area of each class instead of a single pixel, it introduces small variations of the class, with some shadow and other lighting conditions.

These areas should be stable trough time, this is validated by visual check both on the satellite data itself and validation on the high resolution aerial data that is available every year. For every class 10 different areas of 10 by 10 meters are selected where the area is homogeneous for a certain class. These are drawn over the imagery, and saved as a shapefile to be imported into the model training. These shapefiles have the same coordinate system as the input imagery to ensure the geographical location of the training areas will always refer to the exact same area for every input image.

Figure 4.2: Example from training dataset, light-green square top left is 10 by 10 meter training for the grass class, bottom right brown square is a training square for tree class.

4.5 Classification models

There is a wide range of classification techniques, from this a selection that can be tested has to be made. This model selection has to fulfil a couple of requirements. First, each method has to work with raster data. Furthermore, it has to be able to output some form of likelihood of a pixel belonging to a class, this so-called fuzzy classification (Chiang and Hsu, 2002) could be seen as which percentage of the pixel is filled with each class. The last requirement is that the method has to be able to work with several input layers of data.

The selection of our models goes from simple till complex. For the more complicated models there will be more parameters to be optimized and these models will therefore take longer to train. This complexity will hopefully be offset by more accurate results that are more useful for the monitoring task. The three methods in Table 4.1 will be considered:

Model name	Class decision	Fuzzy classification
Nearest Centroid	Closest class centroid	Distance to centroid
Random Forest	Chosen by most trees	Number of trees
Neural Network	Highest weight in output node	Weight of each output node

Table 4.1: Classification models considered in this research, with basic explanation of how the model functions.

4.5.1 Nearest centroid

The first model is the simplest of the considered models, it is a distance based algorithm, (Gou et al., 2012) The first step is finding the centroid of the features of the training data of each target class. The centroid is defined as the mean of the features of each training class, there are as many centroids as there are training classes. The construction of these centroids is a relatively simple operation which scales linearly with the amount of training points (Schütze et al., 2008).

To get a classification for a point, the distance of each point is calculated in feature space to each centroid. The centroid at smallest distance is most likely to correspond to the class that that point belongs to, so this distance is used to get an estimated likelihood that the pixel belongs to that class. This likelihood is scaled by total distance to all the centroids and then inverted, the formula is in 4.1.

$$likelihood_{class1} = 1 - \frac{d_1}{d_1 + d_2 + d_3} \tag{4.1}$$

with:

d_i = distance to centroid of class i

The visualization in figure 4.3 shows how this works for a 2D feature space. In this example the value of the training data of each feature/band is averaged per class. This average will be the centroid of this class. To classify any pixel requires one searches for the closest centroid to the values of that pixel in feature space.

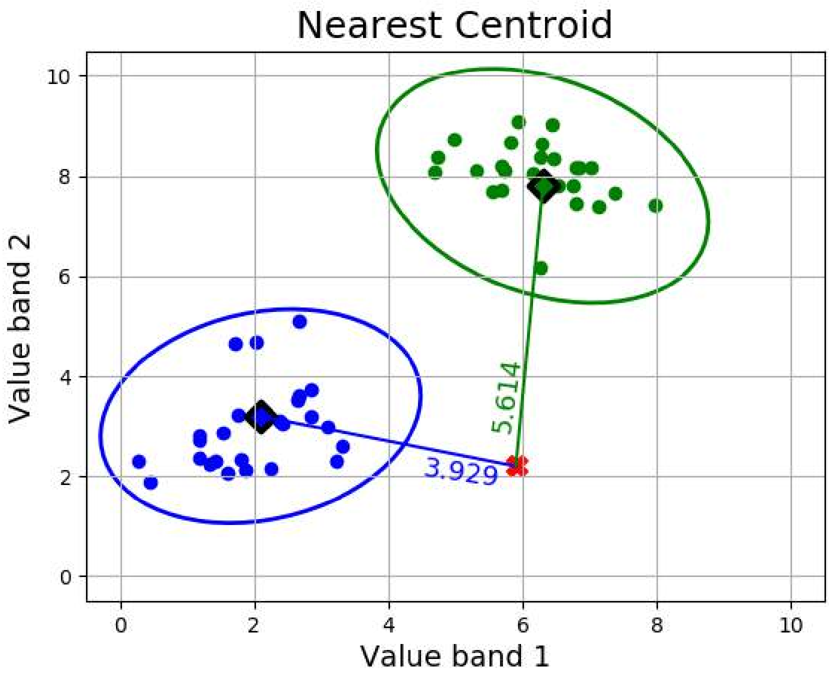

Figure 4.3: Nearest Centroid example in 2D Features space, two classes values put into feature space, centroid of each class marked by diamond, new point displayed as red cross, distance to each centroid is calculated, point added to class of the closest centroid

4.5.2 Random Forest

The random forest model (Breiman, 2001) is a method that combines multiple decision trees into an ensemble. One such decision tree makes binary choices in the feature space to get the best splits. The best split is identified by using the gini impurity, which uses the probability that a random element is given the incorrect label according to class distribution, (Breiman et al., 1984). By splitting the feature space by consecutive above/below cuts a decision tree is created whose leafs correspond to the target classes.

Eventually all the data in the training data will be totally separated and every datapoint will have its own spot. However this might result in less than optimal results in the final classification as pixels have to be very similar to the trained data, this is called overfitting to the training set. This is mitigated by for example only allowing a certain number of splits per tree or by using a minimal number of training per node. An example of one decision tree is shown in figure 4.4.

The random forest model uses this simple tree design and repeats a certain number of times. By selecting some subset of the training data or a random split for every tree it results in a different decision for each tree. By counting for each class how often it is chosen, by a random forest ensemble, of, say, 100 trees, a final decision can be made. The class for which most tree votes is the class the pixel is assigned to. And the percentage of trees voting for each class can be used to estimate the certainty of that class in the model.

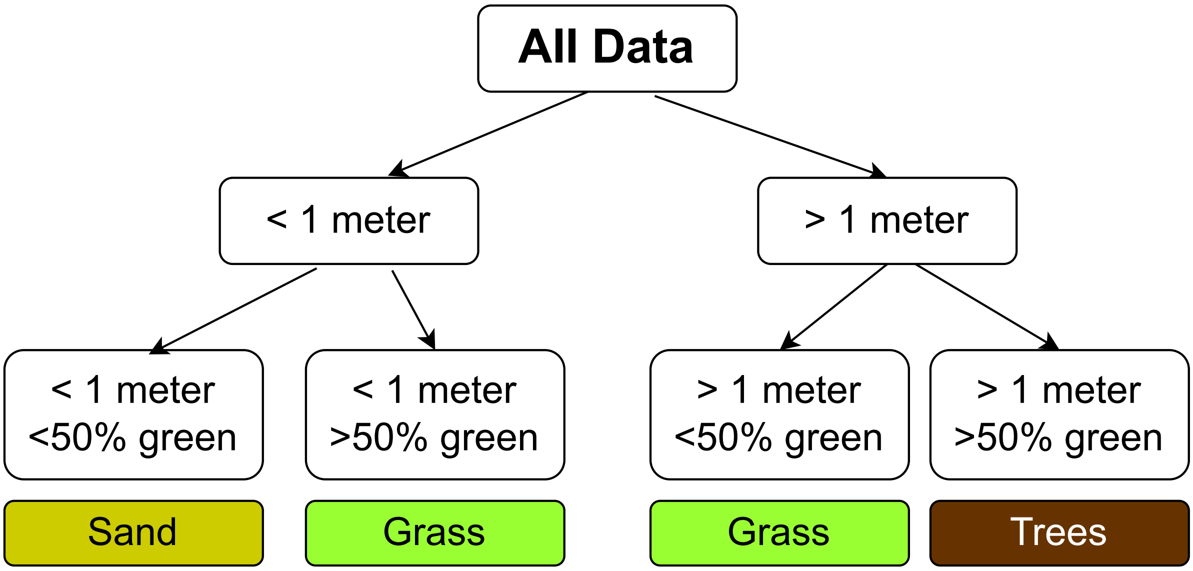

Figure 4.4: Example of decision tree, each split down can have different decisions

4.5.3 Neural Network

A Neural network is a type of machine learning model, based on the concept of how neurons in brains learn. It is one of the most advanced classification methods available, it was implemented using the Tensorflow (Abadi et al., 2015) library in Python. These models consist of at least three layers, the input layer, one or more hidden layers and one output layer. Each layer consists of a number of neurons (or nodes) which are connected to all or some of the neurons from the layer before and the layer after. These connections all have a modifiable weight (or strength). This value will be used by the model to learn. (Wang, 2003).

The number of input nodes is equal to the number of data sources that are put into the model. The part with the hidden layers is the where the model does the work, for this part a number of choices have to be made. The number of layers, the number of nodes and an activation function. These numbers have no perfect answer, as for the number of hidden layers, one is often enough. For the number of nodes there is no real theory for the optimal number, and is thus a setting that requires a bit of experimentation. An visualisation of a neural network is shown in 4.5.

The activation function uses the weight of each input connection to determine what the node will output. For this function there are a lot of possibilities, for example, the sigmoid function is an often used one, but arc tangent and hyperbolic tangents are other often used functions. The last layer contains the output, which can consist of one node where only binary problems

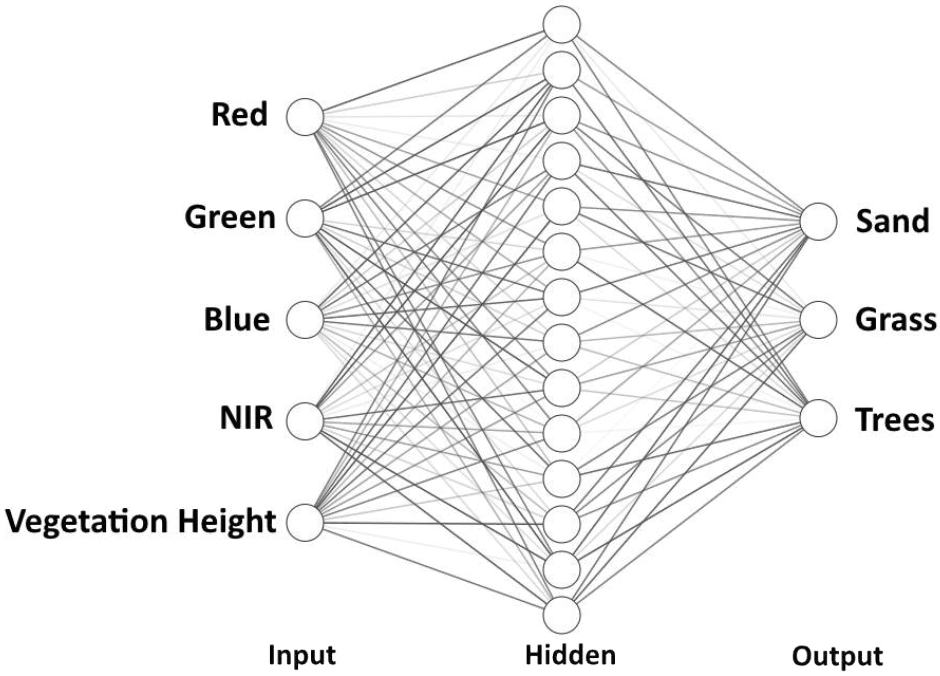

Figure 4.5: Example of a neural network, with 5 input nodes, 14 nodes in the hidden layer and 3 output nodes. Connections between nodes are shaded based on weight.

can be solved. However, in our case, the number of outputs will be equal to the number of classes, and a softmax activation function is used, which is best suited for categorical outputs.

To train the neural network the weights of all the connections between the nodes have to be optimized. This requires a large training dataset, that the model will use to find patterns between the input layers and the output in the training dataset. The progress is quantified by an error function that estimates the difference between the neural network output and the training data, often in the form of a sum of squared errors. The final output will have a value at each output node that is similar to the probability that the input belongs to that nodes class.

4.6 Classification products

All the classifications give a classification per pixel. These than have to be compared and made into a presentable version.

4.6.1 Classified Maps

The most direct result is a map that shows for the whole area which class belongs to each pixel. This result can be made for every date where a satellite image has been taken. This map has no direct indication of how certain the model is of each result. And how within each cell the classes are distributed, where multiple classes could be within one pixel region.

4.6.2 Probability

To get an indication of the certainty of the model for each point, a probability map is made. The map shows if the model was certain that the pixel belongs to this class, or that the pixel is similar to two different classes. This probability is not the same for the three models we consider, with some gravitating to a single class only, while others almost always stay between classes.

This probability can also be used for more fuzzy classification like in Zhan et al. (2000), where extra classes are defined based on the percentage of each class. These extra classes are then used to explore if the methods can see more gradual transitions. For example an class where both grass and sand are likely, which might mean an pixel where the process of transitioning between the classes is taking place.

4.6.3 Timeline generation

One of the biggest strengths of the data we use is the temporal continuity of the data, most dataset have data from multiple timestamps available. By using this temporal information, processes can be made visible and possible errors in classification can be found. To create this temporal overview all the data has to be put into a continuous timeline, which has to account for the irregularly spaced timestamps and missing data points. Then for each pixel the classification over time may be analyzed.

4.7 Accuracy assessment

The accuracy of each method is generated using a training and test dataset. These are constructed by splitting the data. 30% of the original training set is not used to train the model, this is called the test set. This test set is used to calculate several statistics for each model. Using these statistics the models is evaluated and their performance compared.

The statistics show how accurate the model is overall, but also show per class to see if some models work better on certain classes.

The first statistic is the confusion matrix (Foody, 2002), that gives insight in which classes the model has difficulties with. Furthermore, by comparing what the model classifies the pixel to what it is according to the training data, an overall accuracy is calculated. Two other statistics that are calculated from the matrix are the precision and recall. These give insight in if certain classes are found more often than expected or classes where only a small amount are recognized as the correct class.

4.8 Conclusion methodology

In this chapter the workflow of the classification was explained, starting with the preperation of the data for classification. Then the classification models are introduced, three classification methods were explained. The methods are nearest centroid, random forest and neural network methods. These methods represent an scale from easy to understand models till state-of-the-art models that are more difficult to tune.

These classification methods are then used to produce several products that are useful for the vegetation assessment. These products are also used to compare and validate the models. The results will be shown in the next chapter.

5 Results

5.1 Introduction
In this chapter the results of each model will be evaluated. First the models classifications are used to show what the final class labels would be using each method. After this the probability of each classification is shown, this is a parameter to assess model stability or be used for fuzzy classification. As the data has multiple points in time, these points are compared to find trends in the area.

The classification starts with an overview of how the method performs over the whole area. Last, the temporal evolution of three case studies will be discussed in depth.

5.2 Classification
For all three models, a land cover classification, a probability map and a land cover timeline are provided. In Chapter 4, for every model it is explained how to get this probability per class. The underlying probabilities will be shown, which are retrieved directly from each method. This can be used to indicate areas that can not be attributed to a single class.

Including all maps from every method for every date would result in an overload of figures. Therefore only the classification results based on the SuperView data of 2021-09-07 will be shown. This date has the best data quality from the most recent imagery. This is combined with the AHN4 height converted to vegetation height, this is the most recent height data. Classification results for other dates can be found in appendix A.

5.2.1 Nearest Centroid
The classification using the nearest centroid is the closest centroid of the classes in the training dataset to the pixel. This method is therefore dependent on the training as the centroid of the training is used to find the best fitting class. This method only dependents on how the distance is calculated. Here, for this method the Euclidean distance is used for all the input variable. Every point will have 5 distances, one for each input, which are all of equally weight, the closest centroid is at the shortest distance.

Class
The classes with the highest probability, as decided for by the nearest centroid method, are shown in Figure 5.1. The figure shows that grass is identified in large areas. This is likely an overestimation of the amount of grass, as the different vegetation classes (grass and trees)

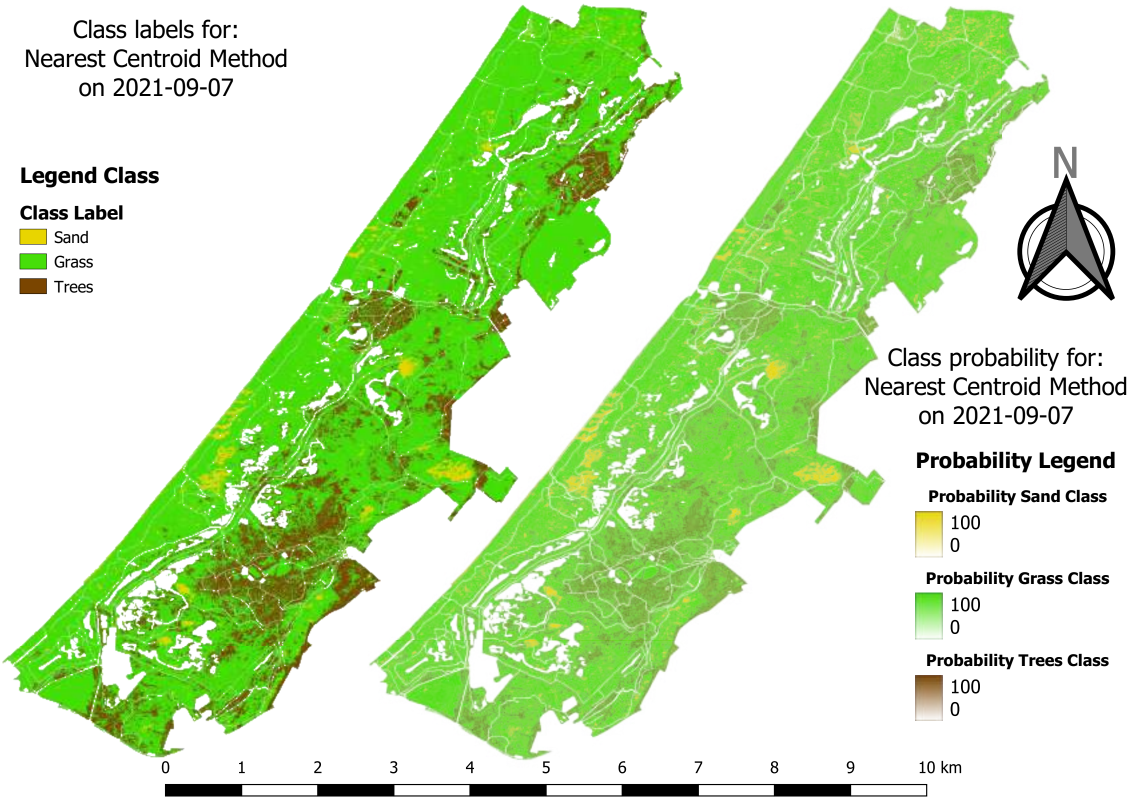

Figure 5.1: Left: Classes according to Nearest Centroid Classifier on Superview satellite image of 7 September 2021. It shows more grass is classified than expected because the border between grass and sand tend to be more often classified towards the grass class.
Right: Probability of each class using Nearest Centroid on Superview satellite image of 7 September 2021, pixels with lower probability will become lighter. This shows that the method has relatively low probability for all classes, because every point has at least some probability for every other class.

Nearest Centroid		Training set			
		Sand	Grass	Trees	User accuracy
Classification data	Sand	460	0	0	100%
	Grass	0	540	0	100%
	Trees	0	85	515	86%
	Producers accuracy	100%	86%	100%	95%

Table 5.1: Confusion matrix for the nearest centroid method

are mostly separated by the vegetation height map. A bush with a height closer to the ground will be closer to the average height of the grass class than the high average of the tree class.

The grass and sand class work quite good on just sand or clear grass. Any vegetation cover between grass and sand will mostly become classified as grass as this pixel will be darker than clean sand and therefore much closer to the grass class. This means the total amount of sand is much lower than expected because only the purest form of sand class is classified as sand. However, as can be seen in the confusion matrix in table 5.1 the method has difficulty classifying between trees and grass, with some grass being classified as trees.

Probability

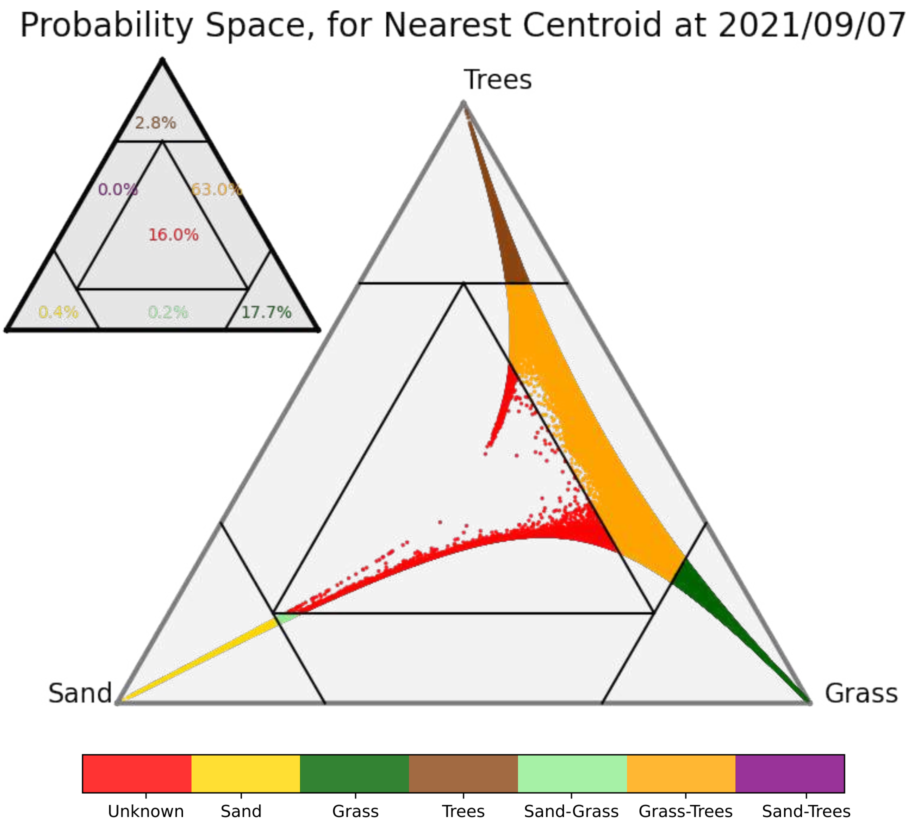

Figure 5.2: Fuzzy classification according to probability by Nearest Centroid, plotted with border to find fuzzy classes between the pure corners. The Nearest Centroid method will always result in a probability for all three classes. This causes classes to be classified to the center class, where all classes are equally likely, more often. As can be seen in the small triangle a high percentage of points is put in the grass class and the subclass between grass and trees. Whereas the subclass between sand and grass is mostly empty.

The probability of the nearest centroid model follows a quite striking pattern, as can be seen in the probability graph in Figure 5.2. This pattern is caused by the fact that only pixels that are very close to a centroid will get a high probability. Any point that is further from the centroid of its class, will come closer to the centroids of other classes. And because the centroids of the grass and trees class are closer to each other than to the sand class, the subclass between grass and trees will be filled more.

5.2.2 Random forest

The random forest classifier is as the name predicts a random classifier, therefore every result will be slightly different each time the training is done. The settings used to get these result are a max tree depth of 10 to stop the overfitting of the model to the training data.

Class

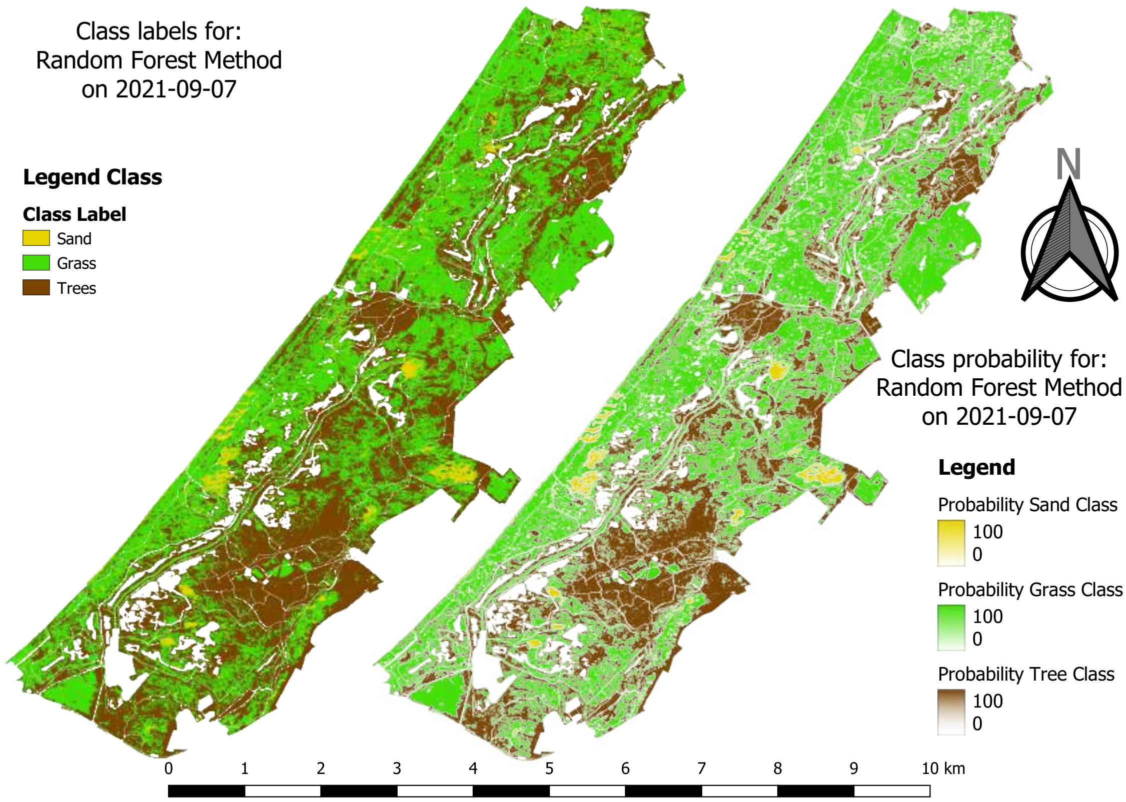

Figure 5.3: left: Classes according to random forest Classifier on Superview satellite image of 7 September 2021. Much more trees than Nearest Centroid, visually looks clear.
right: Probability of each class using random forest on Superview satellite image of 7 September 2021. High probabilities except for borders where lower probability is expected as some trees will have different outcomes

The random forest classified much more pixels to the forest class than the nearest centroid method. The sand class is still easily classified as it has much different characteristics than the other classes. The grass and trees class are classified accurately to the training set, this might give another impression than the visual result implies. This is because the borders between classes are the most difficult to classify, but also the most difficult to verify.

Probability

The probability distribution, Figure 5.4, of the random forest method shows that the vegetation classes can be separated fairly well from the sand. However the subclass between the grass and trees has more points, suggesting that the separation between these classes is less crisp. This means that a part of the trees in the random forest got to the grass class and another number of trees got to the tree class. And between sand and grass there will be a border where some pixels will have factors of both class in them, resulting in some pixel falling in there.

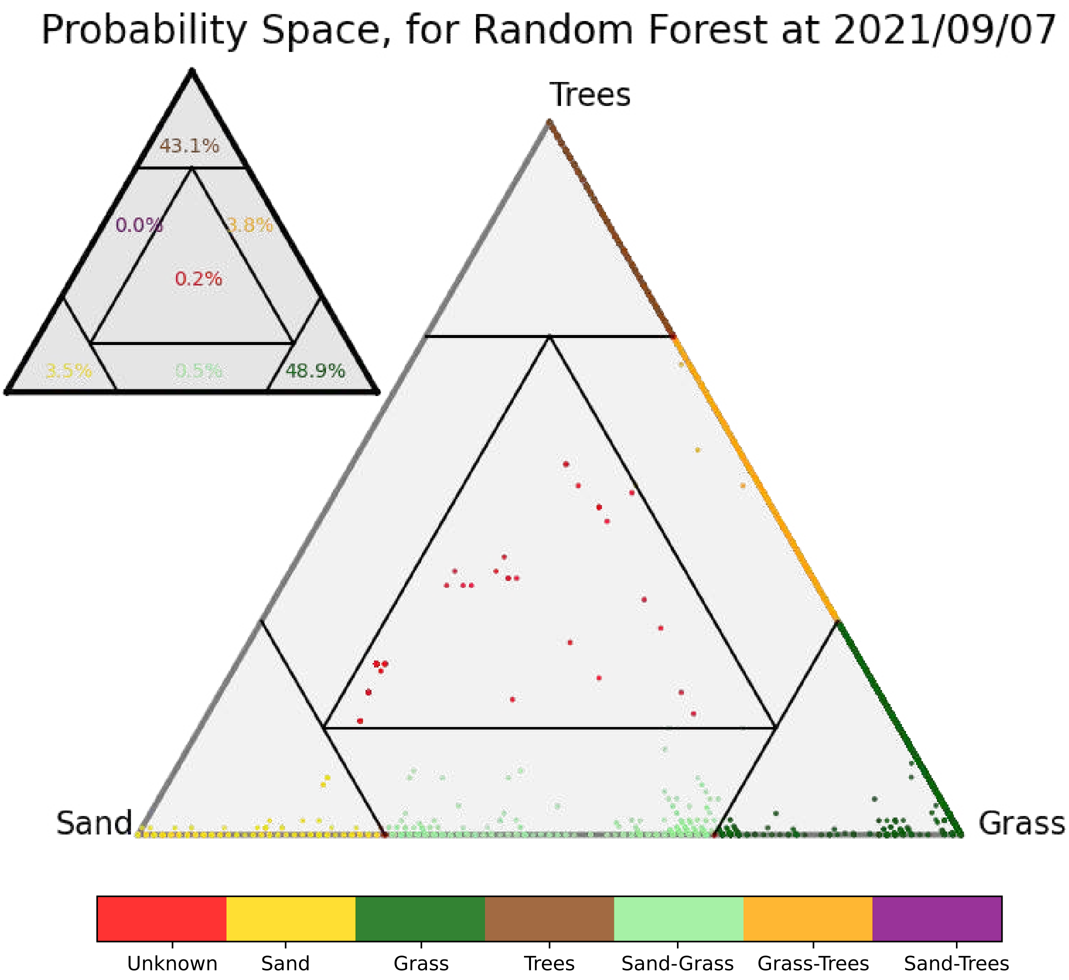

Figure 5.4: Fuzzy classification according to probability by random forest, plotted find sub-classes between full classes. Trees class all far away from sand, linear pattern can be caused by certain division in trees.

Random forest		Training set			
		Sand	Grass	Trees	User accuracy
Classification data	Sand	460	0	0	100%
	Grass	0	537	3	99%
	Trees	0	7	593	98%
	Producers accuracy	100%	98%	99%	99.4%

Table 5.2: Confusion matrix for the random forest method

5.2.3 Neural Network

The neural network is the most advanced model, It is therefore difficult to tune to the best settings. The results will therefore always have some sort of random result as the tuning has to stop overfitting to still get reliable results on the test data. For this result a model with one hidden layer composing 14 nodes is used, these nodes use a relu activation function. While the nodes in the output layer use the softmax activation function. This model is trained for 25 epochs, to increase the categorical accuracy of the model.

Class

The classes as classified by the neural network are shown in Figure 5.5. The result is very similar to the result of the random forest. However, there are some small differences, the Neural network predicts a bit more tree class. This might be explained by classifying some bushes into the tree class. The transition point between the grass and sand is slightly differently than in the other methods. However, the pure classes are classified similarly as the random forest method, this can also be seen in the confusion matrix in Table 5.3.

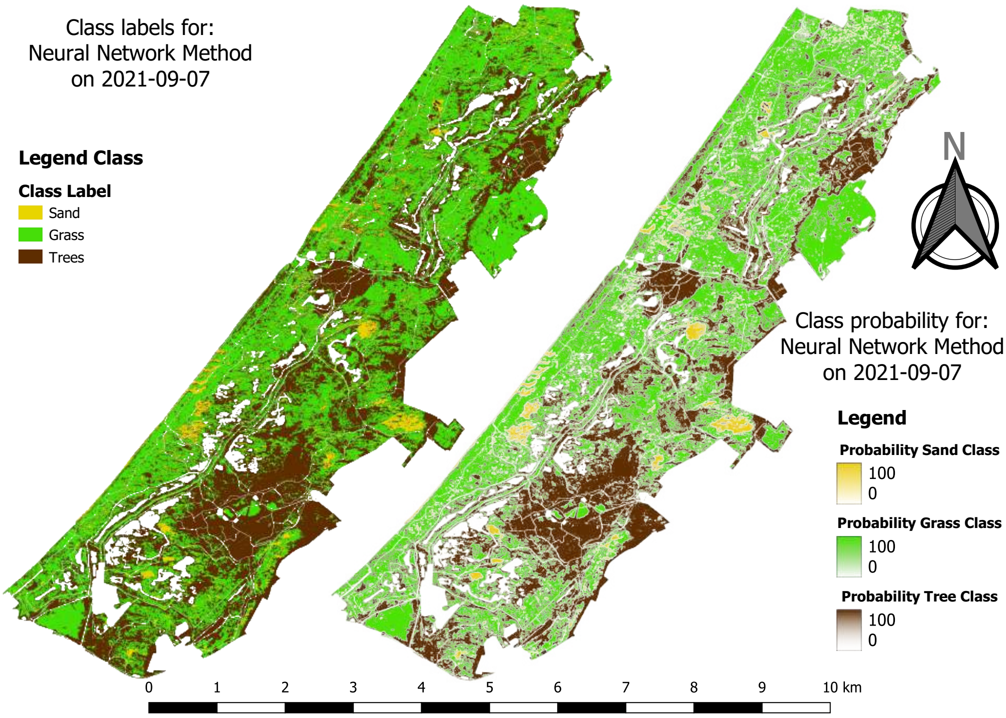

Figure 5.5: left: Classes according to Neural Network on Superview satellite image of 7 September 2021. The result is very similar to the result of random forest (Figure 5.3), with differences concentrated at the edges of classes.
right: Probability of each classes based on the Neural Network on an Superview satellite image of 7 September 2021. Very few places with low probabilities, causing the image to look very similar to the final classes

Neural Network		Training set			
		Sand	Grass	Trees	User accuracy
Classification data	Sand	460	0	0	100%
	Grass	0	528	12	97%
	Trees	0	4	596	99%
	Producers accuracy	100%	99%	97%	99%

Table 5.3: Confusion matrix for the neural network method.

Probability

The probabilities of the neural network are the weights given to each end node. The model is optimised to be as certain as possible, this means most pixels will have a single, very high, probability. The borders between classes will therefore be quite thin and most probabilities will be quite high. The probabilities in the right of Figure 5.5 will therefore look quite similar to the class result.

In the probability distribution in Figure 5.6, it can be seen that high percentages occur into the final class corners, while the between classes show lower percentages. However the whole feature space seems to be filled. The emptiest part is the center, which suggest that for most pixels at least one class is eliminated, as it rarely occurs that the neural network predicts that 3 class outcomes are equally likely

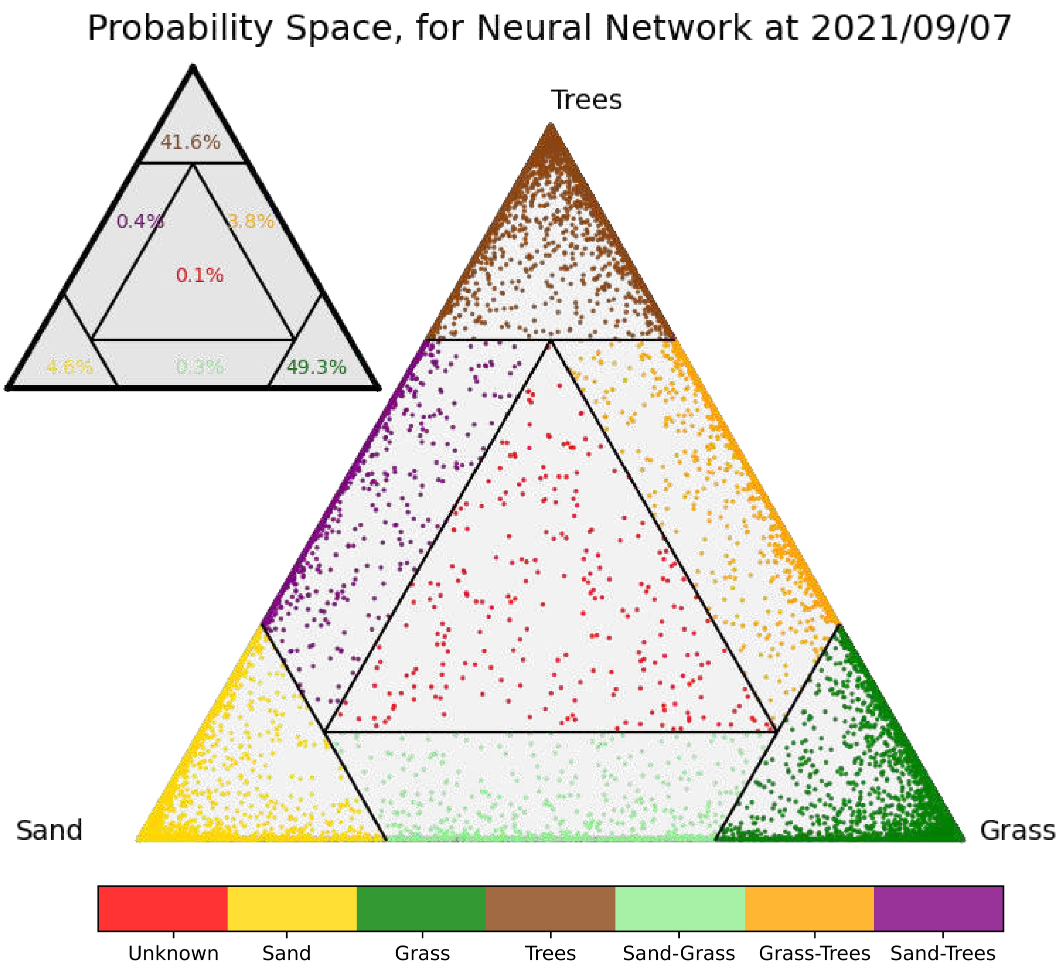

Figure 5.6: Fuzzy classification according to probability by Neural Network, plotted to find sub-classes between full classes. Most points on the corners of the triangle and along the borders, points with lower probability are spread over the whole probability space.

5.3 Fuzzy classification

The classes as visualized by the probability plots, may be used to find sub-classes between the full classes. Classes which include grassy sand, and places where trees and grass are combined in the same pixel. These sub-class pixels are mostly located on borders between different land covers types, these transitions indicate that the between pixels should be seen as partially filled by both classes. This effect can be seen in Figure 5.7. Most fuzzy classes are found on the edges of the pure classes, which makes for a smoother transition between classes.

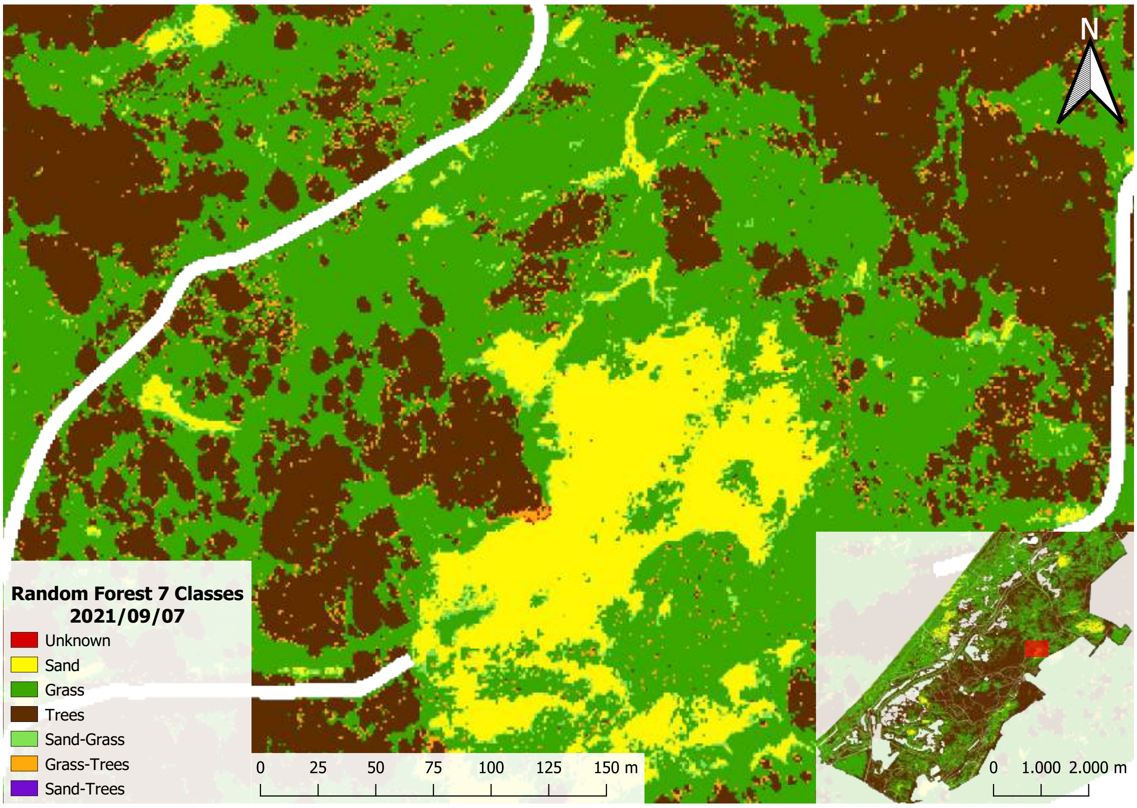

Figure 5.7: Fuzzy classification by random forest, Classes based on probability plot. Fuzzy classes are visible on borders between pure classes, orange pixels on the edge between trees and grass and light-green pixels between sand and grass. Inset map shows map location within wider area.

5.4 Timeline of classes

For the timelines all dates that are mentioned in table 3.3 are used. For every point in time the percentage of pixels that are classified to a certain class are counted, see figure 5.8. This timeline shows the classification throughout time, this shows processes that appear in the whole region. This trend could be used to find seasonal patterns. However as can be seen in Figure 5.8 no large seasonal effect is observed. This might be caused by the short timeline, where it is difficult to spot these longer term patterns.

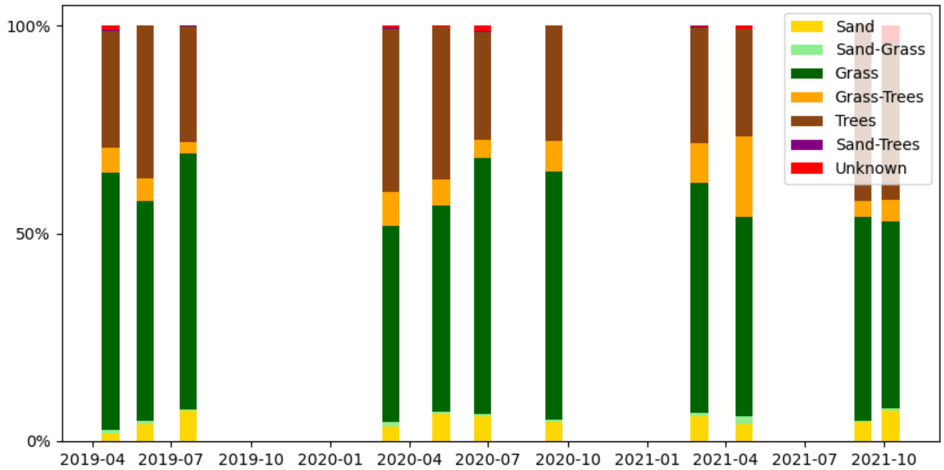

Figure 5.8: Timeline, showing class distribution throughout time for the whole area, based on the Neural Network classification. No strong patterns can be found, might be caused by relatively short time period

5.5 Case studies

In this section several interesting areas will be highlighted. At each of these areas another effect is causing a change in vegetation which are examples of processes that can be picked up by the models.

5.5.1 Transition to grass

This first case is an area where a dune with bare sand has been increasingly covered by vegetation. This is a common process in this type of dunal area (Mücher et al., 2017). As the total time span considered is only about 3 years, the effect can mostly be found at the edges of sand patches. The location of this sand patch is shown in Figure 5.9.

5.5.2 Transition to sand

This case is of an edge of a sand patch on a slope, which can be found through the whole dunal area. This patch has been slowly increasing in size, therefore this point at the edge of this patch has turned from a grassland to an sandy blowout. The location of the classification is shown in Figure 5.11.

5.5.3 Redevelopment of dunes

Larger and sudden changes are the easiest to see, in this case a whole area in the Berkheide area has been cleared of bushes and trees to create new regions for water collection. This project started at the end of October 2020 (Spierenburg, 2020), this can be seen in the timeline in Figure 5.13. The probability in Figure 5.14 shows the clarity of the change within the area.

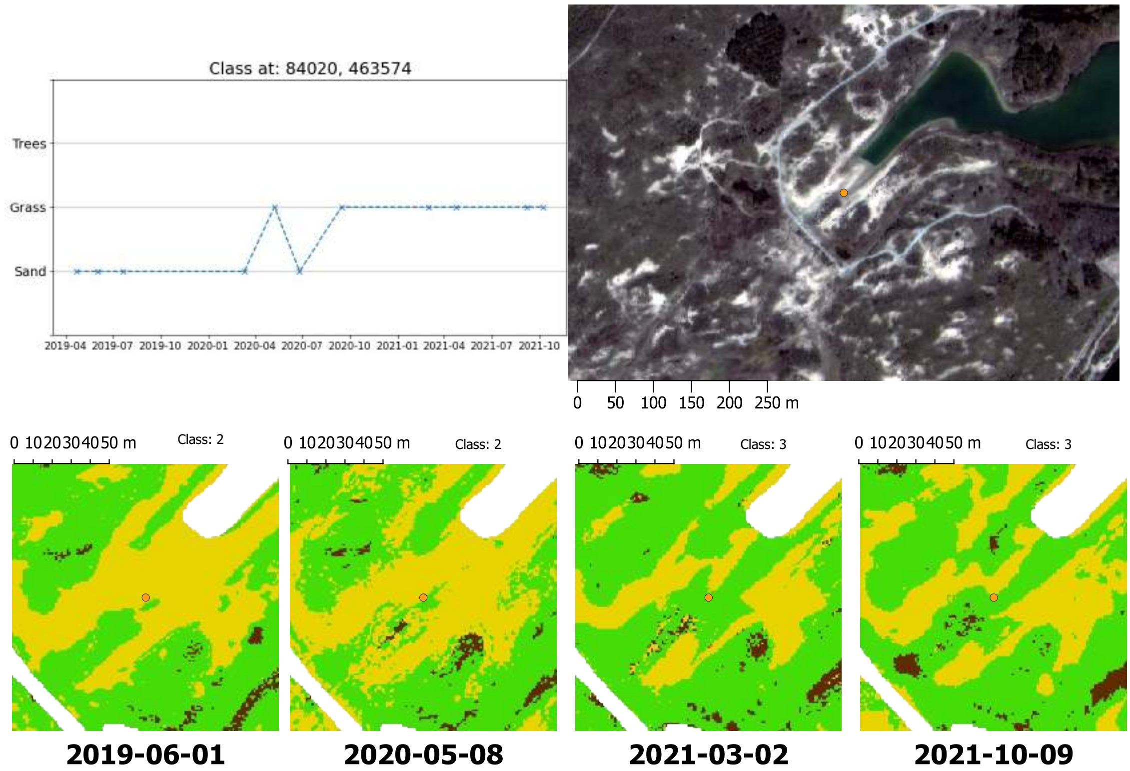

Figure 5.9: Timeline, satellite and four classifications from different time steps of an area turning from sand to grass. The timeline shows that the final classification of the point indicated in the map is vegetation.

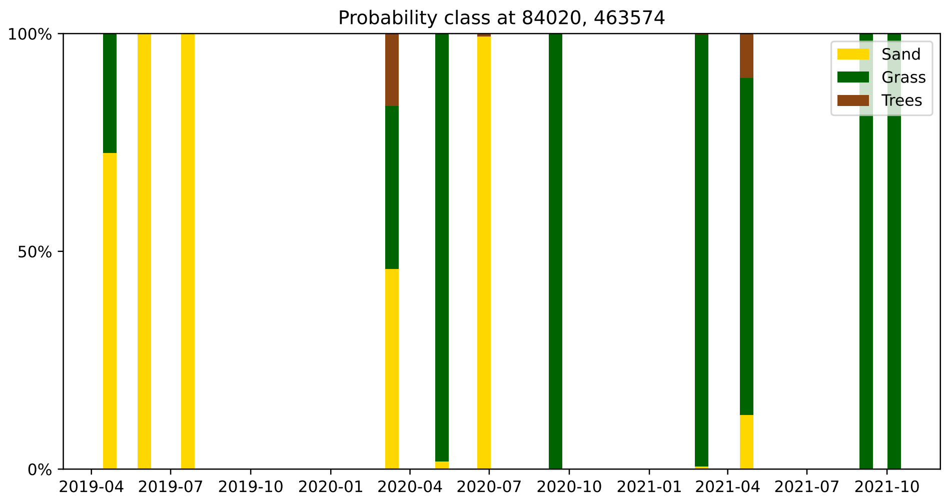

Figure 5.10: Timeline of the resulting class prediction probabilities of the point indicated in Figure 5.9, as obtained using the Neural Network method. High probability for sand is predicted in 2019, some uncertainty occurs in 2020 and a high probability for grass is predicted in 2021.

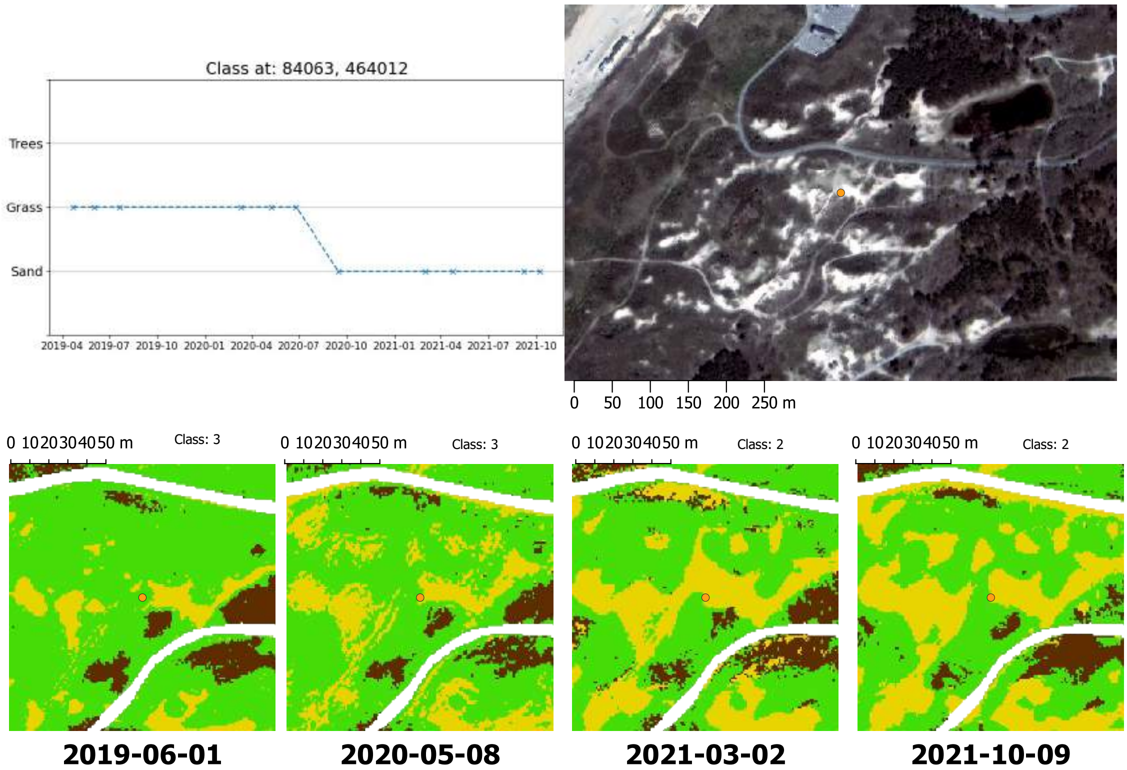

Figure 5.11: Timeline, overview and several time steps class map of area turning from grass to sand. Timeline shows clear transition from grass to sand somewhere in 2020. The location show that the point is located at the edge of a sandy blowout. The 4 classification images show the growth of the blowout throughout time.

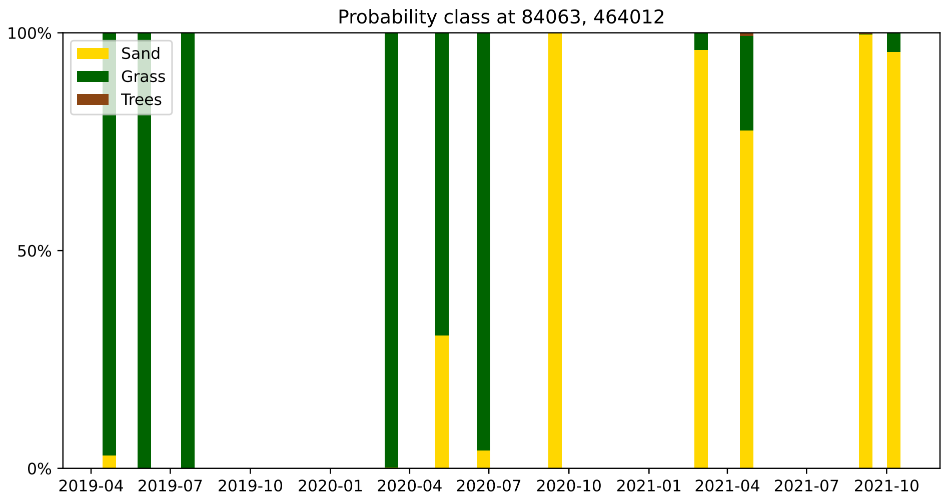

Figure 5.12: Timeline of probability of point seen in Figure 5.11, using Neural Network method. High probability grass till half 2020, after this high probability the pixel turned to sand.

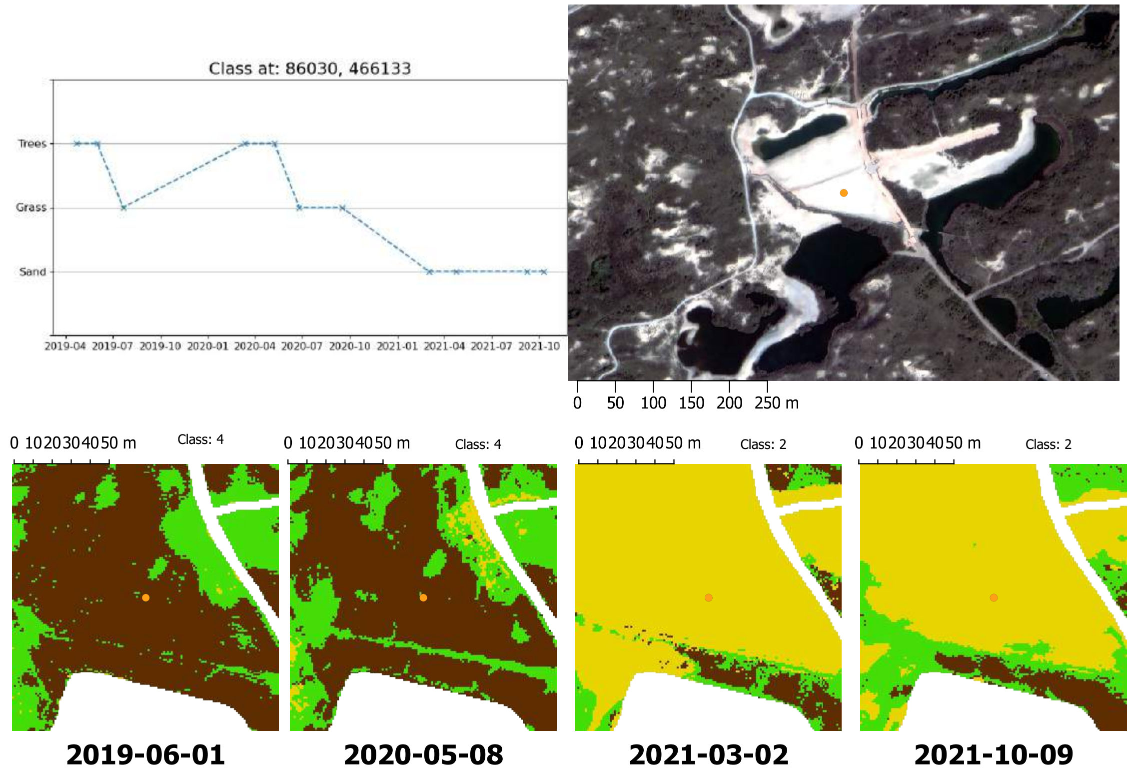

Figure 5.13: Timeline, overview and several time steps class map of area with construction. Timeline shows mostly vegetated before 2020, while in 2021 the sand in recognized. The image shows the location within the new large area of sand. The classification images show the difference between the situation before 2020 and the situation after the re-development had finished.

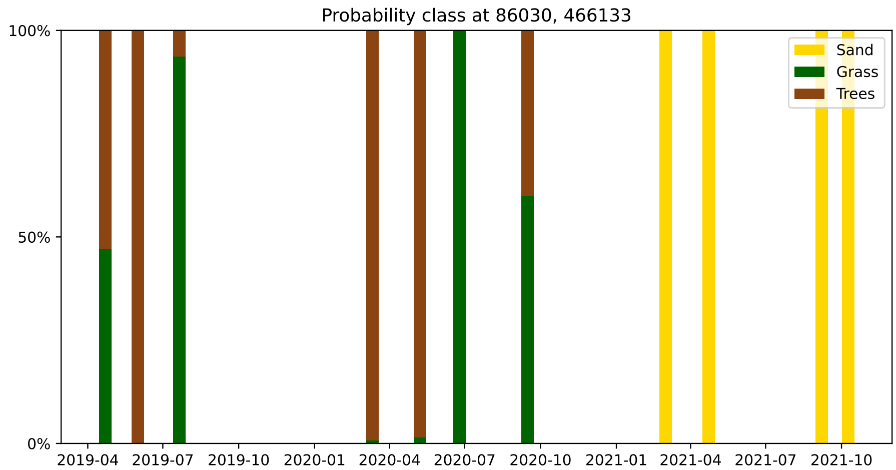

Figure 5.14: Timeline of probability of point seen in Figure 5.13, using Neural Network method. The probability flipped after 2020. From vegetation somewhere between grass and trees to classification 100% certain of sand.

5.6 Conclusion Results

All methods are able to classify the area for vegetation assessment. The nearest centroid method is a simple method, this method shows problems with class transitions and the fuzzy classification does not work for this model. The random forest method and the neural network method seem to perform comparable, their confusion matrices both indicate good results. However random forest method has better identification of what is going on within the model. While the neural network is faster, the method pushes each pixel into the 100% class probability resulting in an non optimal fuzzy classification.

6 Discussion

This chapter discusses data availability, methodological issues and results from a wider perspective. It starts with a discussion on what data was used and what influences the choice for data. Then the methodology is discussed, what has to be considered before using certain models and how to train. Then a discussion follows about how results are shown and difficulties with the accuracy.

6.1 Data Quality

The quality of the final product and before even the processing starts, the quality of the input data influence everything. This quality is partly based on the satellite equipment itself, for example the imagery sensors used. However these raw images will get some corrections to improve certain effects that are caused by taking these images. These corrections can improve the usability of the image, however some corrections can also remove information captured in the original image.

One of the biggest influences are the atmospheric effects on images from space. The radiation has to travel the whole atmosphere causing effects based on atmospheric conditions. This effect has to be corrected for, to reflect more accurately how the condition on the ground is. This process involves whole measurement campaigns, that compare ground measurements with measurements of the satellite. For the Superview satellites, this campaign is described in Liu et al. (2020).

The image has to be placed to an actual location, this location has to be accurate for every image. This geographical placement can be deduced from the known orbit of the satellite. Other ways are using known locations on every image, this method is more accurate but costs more time to do. Also the coordinates of the location have to be same, by making these the same for all datasets, all the images will be exactly on the same location.

Another process that is being done on the satellite imagery is pansharpening, this combines the color image with an higher resolution monochrome image. In this process the low quality imagery is being interpolated using the monochrome image, this results in higher resolution color images. Interpolation processes always lose some accuracy as the processes estimate using lower quality data.

To assess how valid the resulting satellite images are, they are compared to imagery taken from airplanes. These images are less affected by the atmospheric effect and don't need the pansharpening method to get to a sub-meter resolution.

As one of the factors of the data used for this project is that the data is readily available, continuity in data availability has to be accounted for. This satellite data over the Netherlands is provided by the NSO (Netherlands Space Office), they decided what satellite data to acquire. They do this based on several factors, partly on requests from users. Most of the time this change has been to a dataset with better spatial resolution.

As for the LiDAR dataset these datasets are less available, causing the height input to be similar over longer time periods. A tree class should not dependent solely on being a high point. The update of this dataset might be used to find differences between time periods. However it would be unfeasible to get this type of data as often as the optical datasets.

6.2 Data processing

The processing that has to be done on the data to make it more usable for the classification. For this reason every dataset has to be made to the same specification. As this will make the combination of the datasets possible. For this to work all the datasets have to get similar pixelsizes, the process to do this is resampling. This process combines multiple pixels into one larger pixel, this process loses some information as the information from four pixels is reduced to a single pixel.

Another choice that has to be made is if and how the intermediate progress imagery is saved. Other factors are the accuracy that is required, more bits per pixel means better precision but can also mean exponential more storage needed. For example the storage of an image at 8-bit would require about 100MB, while at the 16 bit it takes up twice as much. This could add up if all the in between steps are saved, and the satellite images with the four bands combined use up about a gigabyte of space per timestep.

6.3 Computational challenges

Working with satellite data requires a lot of computing power and storage. For the reason of ease of use all the models should on consumer hardware. Dependent on the type of hardware and the actual model used the time it takes to run will be different. Also some of the parameters can be set to make it computationally easier and require less processing time.

With the amount of data that will be used, the computer would benefit most from fast access to storage. This access would improve each model as each model needs some data access, however each model has different amounts of time that the data needs to be accessed. Some models also support some form of parallel work, this separates the work into steps that can be done simultaneously.

For an insight in how the models compare to each other in time, the processing time for each of the models has been compared. The computer uses an Solid-State Drive for fast access to the data. The CPU that is important for the processing is an AMD 5900x, with a clock speed of about 4.5GHz. The amount of memory available is 32GB, this is able to save the dataset for very fast access while the classification is being done.

As can be seen in the table 6.1, the nearest centroid model is much faster but results in worse accuracy. The difference in time between the random forest and neural network might be explained by the efficiency of each of the implementations of the models. Neural network is more often used for big data sets where the whole model is better optimized for parallel processing. Also the memory usage for the random forest method is not optimal, restricting the amount of trees that can be run simultaneous parallel steps.

Method	Time taken
Nearest Centroid	40 seconds
Random Forest	210 seconds
Neural Network	100 seconds

Table 6.1: Approximate time requirement per method for one timestep. The time required is dependent on the hardware used and the exact implantation of each method.

6.4 Training

The training data used for the results has only three classes, the sand, grass and tree classes. These are the important coastal vegetation classes, with a logical progression from bare sand, to grass and finally to trees and other bushes. However the most interesting parts is the transition between the classes. One way to obtain these transitions is comparing if the classification result transfers between classes through time. This method is only able to tell this after several time steps. An other method is seeing how likely each class is according to the prediction model A pixel that is equally likely belonging to sand as to grass, is probably halfway between the classes.

This method is based on the assumption that the progress is linear, and is difficult to validate. The way to validate this would require in-situ observation data that include estimations how far a point (or rectangle) between the sand and grass class is. This might be done by defining classes between the pure classes, or points that include percentages for each class. These points should be acquired often enough so that these points are still in the same condition on the next satellite image.

6.4.1 Alternative Training sets

These classification methods are specially designed for the vegetation in coastal area's. For a more general classification more classes could be added to the training set. The amount of classes needs more time to create the training data in the field and the training of models will take longer.

Examples of additional classes are objects like water and specific vegetation species. Water could be made into a class to be classified by the model, this is useful for area's with more dynamic water features or without any good quality, up to date water masks. The water class are mostly stationary classes which don't move within our time period. However longer time periods might require several water masks through the period. Addition of classes might turn the actual vegetation classes in shadow pixels might be mistaken as the water class. Including these classes might worsen the accuracy of the vegetation that is the priority of our classification. Therefore these were masked in our methodology.

6.5 Examination of model results

In the results of the models, at certain edges of classes the first traces of processes can be seen. The certainty that these processes are actually occurring and not just classification bias could be increased by using data from a longer time period. For our case this would mean using data with a lower spatial resolution, with pixel size of more than one meter. This would however make it difficult to create a consistent timeline as resolution changes. The clearest results are in the area where abrupt processes occur, like the clearing from vegetation of an area. These processes are a lot less common and are also often at known locations.

6.5.1 Continuity of classification

The model could take the surrounding time steps results into account to smooth out change. This means that the pixels do not change between classes as often, but makes changes a more gradual process. However, relying on past results can also hide actual change, with seasonal effect being dampened.

The pixel-based classification could be improved by taking into account surrounding pixels in the classification. This makes edges less direct, but creates a more likely classification as the surrounding vegetation has influence on the likely vegetation in the pixel. This could be done by adding averaged layers, which also need storage and add to the processing time. The advantage of the information of these surroundings could make for a more gradual edge at the cost of processing time.

6.5.2 Probability to new class

The transition classes need a value at which the classification does not belong to the pure class anymore. The location of these splits is subjective, as making the split at a high probability will result in pixels with small disturbances being put out of the pure classes. While a split with low probability will have almost no pixels in the transition classes. The split could be different for every method and maybe even for every time step as the effects of light and how the probability is estimated all have effect on these class distribution.

The triangles that are shown in the result use an split of 70% probability. This can be changed for every method separately, as each method has different sensitivity to each transition. To get an accurate split, validation data would be needed on when a pixel would be in transition.

7

Conclusions and recommendations

This chapter summarizes this studies results, explained in the research steps as introduced in Chapter 1. After this a couple of recommendations are made on parts of methodology that could be improved on the classification procedure.

7.1 Conclusions

The objective of this thesis was to explore the feasibility of using readily available remote sensing data for vegetation assessment. As an alternative to the airplane data that is currently in use. These possibilities have been explored on the Meijendel & Berkheide area at the Dutch coast between The Hague and Katwijk.

What are the desired properties of the end-product?
The resulting classification should be comparable to the existing classification based on remote sensing. This means that at least sand and grass should be classified, together with some way to find transition classes, this type of classification is known as fuzzy classification. More vegetation classes could be added for identifying higher vegetation for more information in the state of vegetation. Static classes are less important to classify as the are not expected to change and they will only to make the classification process more difficult.

What suitable satellite and aerial data is readily available for the selected area, time period and application?
There are a lot of high-quality data sources that are made possible by the advances of the remote sensing field in the recent years. The types that were selected are a type of spectral data, especially with a near-infrared band for vegetation, together with some geometric information like height, combined these data factors are able to assess vegetation. To make use of this abundance of data useful the existing methodology is not up to the task. This requires that a new method for classification has to be found, this new method has to be able to work with multiple data sets and use the combined information to classify.

What natural processes can be determined by each data type?
For the dunes an important process is the balance between bare sand and grassland, with places where grass and other low vegetation will overgrow sand patches. As well as areas where sand can still move freely with the wind. By combining classification from several time steps naturally occurring processes in the area can be followed.

How can data from different sources be processed into one combined method?
All the data sources should have the same scale and projection to exclude any problems with datasets not aligning. To find an classification that is accurate over a longer time certain factors have to be considered as not all dataset have to the same update time. The training data should be stable over the whole time period or it could influence the accuracy throughout time.

How can the quality of the final product be determined?
A problem with this stable training is the difficulty of validating the classification. The transition classes are difficult to validate as they change location over time, and to quantify exactly when the transition has happened is difficult. This would require validation field work for each image acquisition.

Three different methods were compared in this study; nearest centroid, random forest and neural network. The nearest centroid method is not adjustable and this results in the lowest accuracy. The random forest method and neural network method performed comparable. Random forest is the less advanced of these two models, which makes it possible to find out what the model is doing. Neural network is a more advanced model, which might produce better result with more tweaking. But it will always be virtually impossible to find out exactly what the model is doing. The random forest model's relatively better performance on the fuzzy classification and the ability to analyse the decisions, makes it the preferable model for the purpose of vegetation assessment for this area.

In summary, the fusion of optical satellite data with LiDAR elevation data is a suitable alternative to the airborne only classifications. Together with the addition of the probability to transition classes improves the usability of the final classification.

7.2 Recommendations

As this is an exploratory research into the topic of vegetation assessment, further research could improve results of the classification in several ways. The data inputs in this paper only used the basic geometrical information of height in raster form. Within the raw LiDAR data more information is available in point form, for example density and intensities can improve classification.

The methodologies that are used in the paper have configuration parameters that influence the classification. Especially for the Neural Network this would require much more knowledge of the model and time to find the most optimal settings. Also the more advanced convolution that includes information of surrounding pixels in the classification could help with smoother results at borders of classes.

Points in the field should be used for training and validation purposes, which will improve the classification and make the comparison more quantifiable. The process for this point gathering would require knowledge of the area and a procedure for quantifying each class for points to be used in the classification.

Bibliography

Abadi, M., Agarwal, A., Barham, P., Brevdo, E., Chen, Z., Citro, C., Corrado, G. S., Davis, A., Dean, J., Devin, M., Ghemawat, S., Goodfellow, I., Harp, A., Irving, G., Isard, M., Jia, Y., Jozefowicz, R., Kaiser, L., Kudlur, M., Levenberg, J., Mané, D., Monga, R., Moore, S., Murray, D., Olah, C., Schuster, M., Shlens, J., Steiner, B., Sutskever, I., Talwar, K., Tucker, P., Vanhoucke, V., Vasudevan, V., Viégas, F., Vinyals, O., Warden, P., Wattenberg, M., Wicke, M., Yu, Y., Zheng, X., 2015. TensorFlow: Large-scale machine learning on heterogeneous systems. Software available from tensorflow.org.

Abburu, S., Babu Golla, S., 2015. Satellite Image Classification Methods and Techniques: A Review. *International Journal of Computer Applications*, 119(8), 20–25.

AHN, n.d. Kwaliteitsbeschrijving Actueel Hoogtebestand Nederland.

Assendorp, D., 2010. Classification of Pattern and Process in Small - Scale Dynamic Ecosystems ;.

Bannari, A., Morin, D., Bonn, F., Huete, A. R., 1995. A review of vegetation indices. *Remote Sensing Reviews*, 13, 95–120. https://www.tandfonline.com/action/journalInformation?journalCode=grsr20.

Breiman, L., 2001. Random forests. *Machine learning*, 45(1), 5–32.

Breiman, L., Friedman, J., Stone, C. J., Olshen, R. A., 1984. *Classification and regression trees*. CRC press.

Chiang, I.-J., Hsu, J. Y.-j., 2002. Fuzzy classification trees for data analysis. *Fuzzy sets and systems*, 130(1), 87–99.

Cracknell, A. P., 2007. *Introduction to remote sensing*. CRC press.

De Boer, T. A., 1993. Botanical characteristics of vegetation and their influence on remote sensing. *Land observation by remote sensing*, 89–103.

de Lange, R., van Til, M., 2004. The use of hyperspectral data in coastal zone vegetation monitoring.

Doody, J. P., 2012. *Coastal conservation and management: an ecological perspective*. 13, Springer Science & Business Media.

Foody, G. M., 2002. Status of land cover classification accuracy assessment. *Remote Sensing of Environment*, 80(1), 185–201.

Gou, J., Yi, Z., Du, L., Xiong, T., 2012. A local mean-based k-nearest centroid neighbor classifier. *The Computer Journal*, 55(9), 1058–1071.

Hantson, W., Kooistra, L., Slim, P. A., 2012. Mapping invasive woody species in coastal dunes in the Netherlands: a remote sensing approach using LIDAR and high-resolution aerial photographs. *Applied Vegetation Science*, 15(4), 536–547.

Janssen, J. A. M., Bijlsma, R. J., Damm, T., van Heerden, A., 2015. Vegetatie-en habitatkartering duinen Meijendel 2011.

Kasampalis, D. A., Alexandridis, T. K., Deva, C., Challinor, A., Moshou, D., Zalidis, G., 2018. Contribution of remote sensing on crop models: A review. *Journal of Imaging*, 4(4).

Kempeneers, P., Deronde, B., Provoost, S., Houthuys, R., 2009. Synergy of Airborne Digital Camera and Lidar Data to Map Coastal Dune Vegetation. *Journal of Coastal Research*.

Lasanta, T., Vicente-Serrano, S. M., 2012. Complex land cover change processes in semiarid Mediterranean regions: An approach using Landsat images in northeast Spain. *Remote Sensing of Environment*, 124, 1–14.

Leimgruber, P., Christen, C. A., Laborderie, A., 2005. The impact of landsat satellite monitoring on conservation biology. *Environmental Monitoring and Assessment*, 106(1-3), 81–101.

Liu, Y.-K., Ma, L.-L., Wang, N., Qian, Y.-G., Zhao, Y.-G., Qiu, S., Gao, C.-X., Long, X.-X., Li, C.-R., 2020. On-orbit radiometric calibration of the optical sensors on-board SuperView-1 satellite using three independent methods. *Optics Express, Vol. 28, Issue 8, pp. 11085-11105*, 28(8), 11085–11105.

Ministerie van Landbouw, Natuur en Voedselkwaliteit, 2005. Habitattypen | Natura 2000.

Mücher, S., Kramer, H., van der Wijngaart, R., Huiskes, R., 2017. Ontwikkelen van een remote sensing monitoringssystematiek voor vegetatiestructuur: pilotstudie: detectie verruiging grijze duinen (h2130) voor het natura 2000-gebied meijendel-berkheide. Technical report, Wageningen Environmental Research.

NSO, n.d. Satellietdataportaal | Spaceoffice.nl.

Rees, W. G., 2013. *Physical principles of remote sensing*. Cambridge university press.

Schmidt, K., Skidmore, A., Kloosterman, E., van Oosten, H., Kumar, L., Janssen, J., 2004. Mapping Coastal Vegetation Using an Expert System and Hyperspectral Imagery. *Photogrammetric Engineering & Remote Sensing*.

Schmitt, M., Zhu, X. X., 2016. Data fusion and remote sensing: An ever-growing relationship. *IEEE Geoscience and Remote Sensing Magazine*, 4(4), 6–23.

Schütze, H., Manning, C. D., Raghavan, P., 2008. *Introduction to information retrieval*. 39, Cambridge University Press Cambridge.

SpacewillInfo, 2020. Superview-1 Satellite Imagery Product Guide.

Spierenburg, P., 2020. Eerste project Programma Berkheide van start. `https://www.dunea.nl/zakelijk/nieuwsbrieven/nieuwsbrief-2020-10/eerste-project-programma-berkheide-van-start`.

Sundseth, K., 2008. Natura 2000: Protecting Europe's biodiversity. 53(9), 1689–1699.

van Beek, J., van Rosmalen, R., van Tooren, B., van der Molen, P., 2018. *Werkwijze monitoring en beoordeling Natuurnetwerk en Natura 2000*. BIJ12.

Wang, S.-C., 2003. Artificial Neural Network. *Interdisciplinary Computing in Java Programming*, 81–100.

Yehia, A., Elhifnawy, H., Safy, M., 2019. Effect of different spatial resolutions of multi-temporal satellite images change detection application. *2019 International Conference on Innovative Trends in Computer Engineering (ITCE)*, IEEE, 41–46.

Zhan, Q., Molenaar, M., Gorte, B., 2000. Urban land use classes with fuzzy membership and classification based on integration of remote sensing and GIS. *International Archives of Photogrammetry and Remote Sensing*, 33(B7/4; PART 7), 1751–1759.

A

Additional results

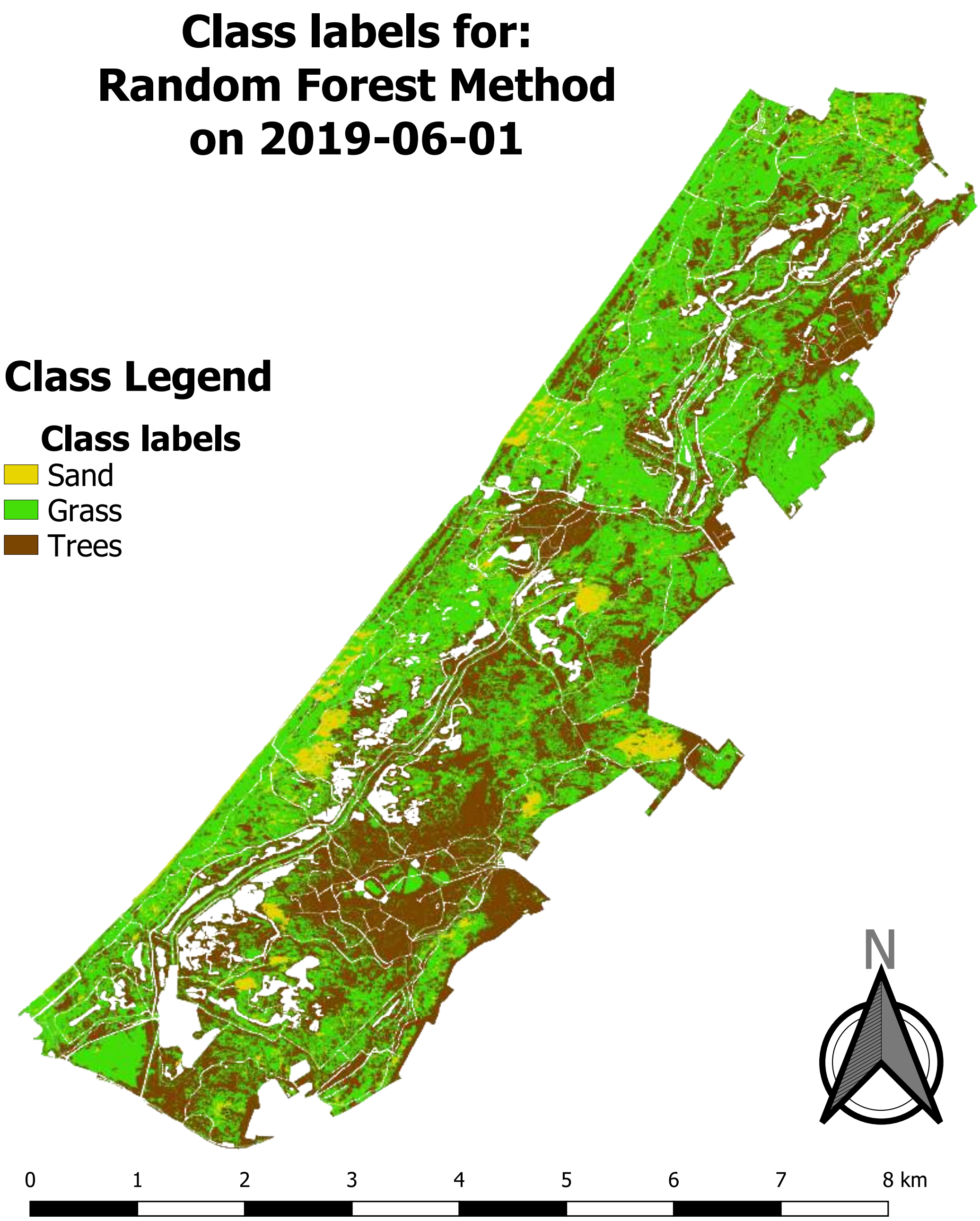

Figure A.1: Class label by random forest method for 2019-06-01.

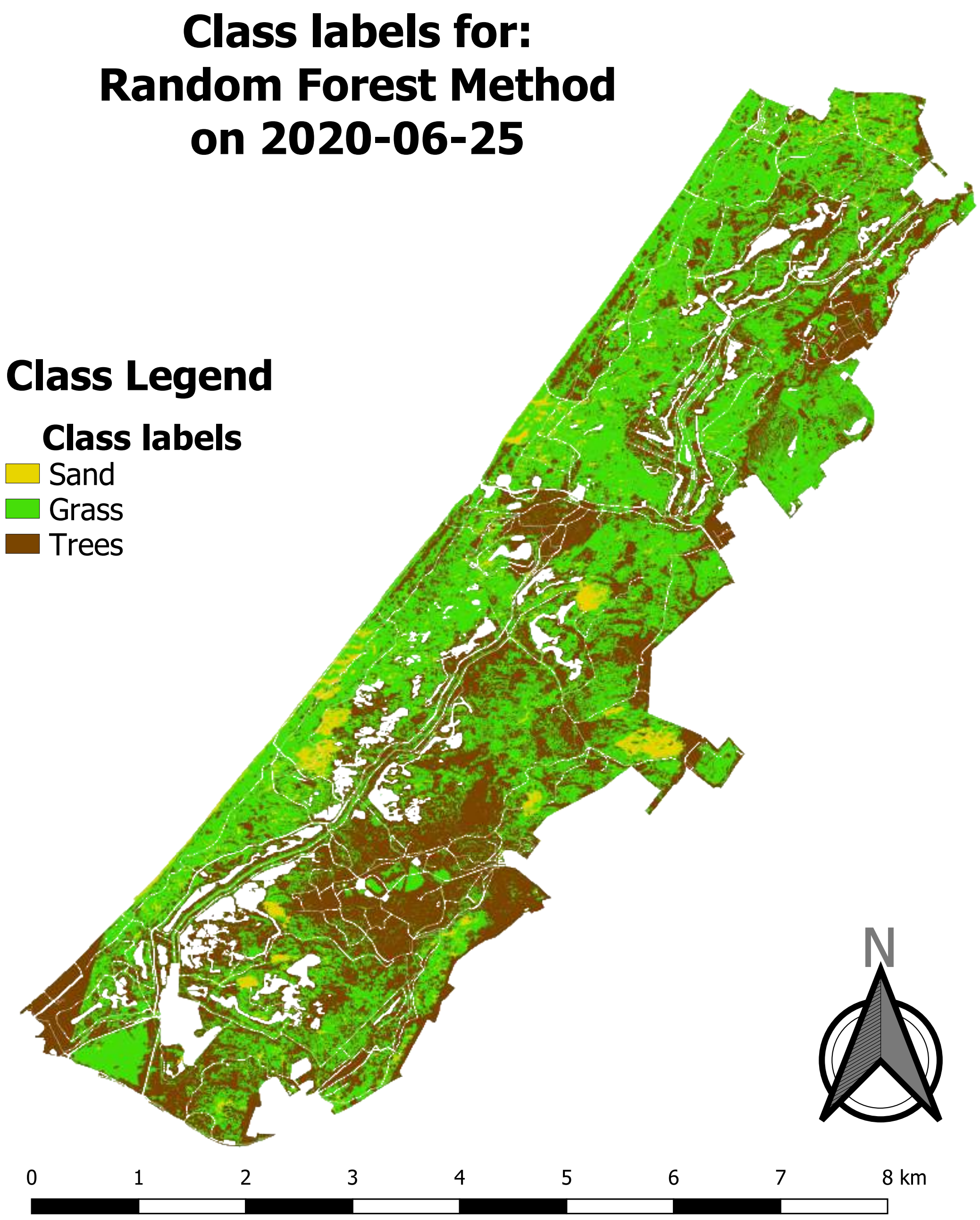

Figure A.2: Class label by random forest method for 2020-06-25.

B

ISPRS Paper

The following paper will be published in the ISPRS Proceedings for the XXIVth ISPRS congress.

PROBABILISTIC VEGETATION TRANSITIONS IN DUNES BY COMBINING SPECTRAL AND LIDAR DATA

H.S. Kathmann[1], A.L. van Natijne[2], R.C. Lindenbergh[2,*]

[1] Dept. of Geoscience and Remote Sensing, Delft University of Technology, H.S.Kathmann@student.tudelft.nl
[2] Dept. of Geoscience and Remote Sensing, Delft University of Technology, (A.L.vanNatijne,R.C.Lindenbergh)@tudelft.nl

WG II/10

KEY WORDS: Habitat mapping, Machine learning, Data fusion, Classification

ABSTRACT:

Monitoring the status of the vegetation is required for nature conservation. This monitoring task is time consuming as kilometers of area have to be investigated and classified. To make this task more manageable, remote sensing is used. The acquisition of airplane remote sensing data is dependent on weather conditions and permission to fly in the busy airspace above the Netherlands. These conditions make it difficult to get a new, dedicated acquisition every year. Therefore, alternatives for this dependency on dedicated airplane surveys are needed. One alternative is the use of optical satellite imagery, as this type of data has improved rapidly in the last decade both in terms of resolution and revisit time. For this study, 0.5 m resolution satellite imagery from the Superview satellite is combined with geometric height data from the Dutch national airborne LiDAR elevation data set AHN. Goal is to classify vegetation into three different classes: sand, grass and trees, apply this classification to multiple epochs, and analyze class transition patterns. Three different classification methods were compared: nearest centroid, random forest and neural network. We show that outcomes of all three methods can be interpreted as class probabilities, but also that these probabilities have different properties for each method. The classification is implemented for 11 different epochs on the Meijendel en Berkheide dunal area on the Dutch coast. We show that mixed probabilities (i.e. between two classes) agree well with class transition processes, and conclude that a shallow neural network combined with pure training samples applied on four different bands (RGB + relative DSM height) produces satisfactory results for the analysis of vegetation transitions with accuracies close to 100%.

1. INTRODUCTION

Nature is an integral part of our environment. In Europe, nature reserves are protected under the Natura 2000 program, (Sundseth and Creed, 2008). As part of this program, habitat development has to be monitored, (Ackerly et al., 2015). Given the vast size of typical nature reserves, remote sensing is an attractive option for monitoring. Remote sensing can be performed in dedicated campaigns, but this is expensive and often complicated to organize. Alternatively, readily available data could be used for monitoring.

The method traditionally used to monitor vegetation transitions in the area of interest is a model called DICRANUM, (Assendorp et al., 2010). This model is based on the red and near infrared (NIR) spectral bands of areal photographs. The red and NIR spectral bands were chosen because their ratio provides the most distinguishing information on vegetation. Classification classes range from bare ground with no vegetation to a class with 100% coverage with shrubs and trees. Between these pure classes, there are 5 fuzzy grassland classes with vegetation mixtures at the sub-pixel level.

In addition, training data is collected for both pure/crisp classes as well as fuzzy classes, (Tapia et al., 2005). The training data is used to identify both crisp and fuzzy classes in the 2-band Red-NIR feature space. The classification procedure results in 6 maps, one with only the crisp/pure classes and 5 with membership values for each of the fuzzy classes. The so-called membership value gives the probability that a pixel belongs to a fuzzy class. A pixel may belong to several fuzzy classes.

* Corresponding author

This fuzzy classification is well suited for vegetation monitoring, (Feilhauer et al., 2021, De Lange et al., 2004). The strength of this approach is its ease of use, and the high accuracy for the crisp classes. However, the disadvantages of the model are the limited information (2 bands) that is used from the input data, as well as the need to acquire field observations to characterize the fuzzy classes in the 2-band feature space.

Given the difficulties to organize the dedicated campaigns, our goal was to analyse to what extend similar or even better results can be obtained from readily and freely available remote sensing products, in combination with state of the art classification techniques that are able to profit from the full bandwidth of available information.

1.1 Area of Interest

The area of interest consists of the Meijendel and Berkheide dunes, compare Figure 1. It is situated at the Dutch coast between the cities of The Hague and Katwijk. The area has a size of 2877 hectares, the southern part is called Meijendel and is the larger area at 1951 hectare while the northern Berkheide is 926 hectare. This Natura2000 area consists of a varied and extensive dune landscape, and is relatively rich in relief.

2. DATA

The remote sensing data considered for this study should be ready to use and relatively up to date. In addition, data should be useful for vegetation characterization. Therefore, it was decided to combine high resolution multi-spectral satellite data with freely available airborne laser scan data, (Kukunda et al.,

Figure 1. Berkheide en Meijendel dune area next to the city of The Hague, The Netherlands

2018) and (Mücher et al., 2015). The spectral data is expected to enable us to distinguish different types of vegetation from notably sand in this area, while airborne laser scan data should be useful in distinguishing high vegetation from terrain. Additional, freely available aerial photos were used for visual inspection. A summary of the used data sets is given in Table 1.

Name	Type	Resolution	Availability
Superview-1	RGBI	50 cm	monthly
AHN	LiDAR	$\sim$ 30 cm	$\sim$6 years
Aerial photo	RGBI	25 cm	yearly

Table 1. Type, spatial resolution and availability of the data sets considered in this study.

2.1 Superview

The Superview satellite mission was launched in 2019 and creates high resolution imagery, (Liu et al., 2020). The data set is provided as a raster, with a ground sampling resolution of 0.5 meters. The imagery contains four bands, with reflectance information in the red, green, blue and a near-infrared bands, (Mozgovoy et al., 2018).

Date	Comments
2019-04-22	Missing SW corner
2019-06-01	Full image, dry period
2019-07-21	Full image
2020-03-11	Slight haze over southern part
2020-05-08	Full image
2020-06-25	Missing SW corner
2020-09-15	Full image
2021-03-02	Full image, low tree cover
2021-04-23	Full image
2021-09-07	Full image
2021-10-09	Missing NE corner

Table 2. Superview-1 data used in this study. Comments are based on visual inspection

The satellite data from the Superview platform, is bought about 6 times a year by the Netherlands Space Office and made available for use by Dutch entities. As this data set is bought for whole swaths of the Netherlands, not all data points are over the area of interest, or of sufficient quality (e.g. cloud cover). This results in about 3 to 5 usable images per year, slightly more often in the summer months. An overview of the Superview images used in this study is given in Table 2. One such image is shown in Figure 2, left. A zoom-in at pixel level is shown in the inset.

2.2 Actueel Hoogtebestand Nederland (AHN)

AHN is a Dutch nation wide elevation model produced using airborne LiDAR, (Van Natijne et al., 2018, Soilán Rodríguez et al., 2019). The elevation model in the raw form is a point cloud, however, for this study the rasterized 0.5 m grid is used. The raster comes in two versions: a terrain model and a surface model. The difference ΔH at a 1m raster between the mean of four terrain heights (at 0.5 m raster) and the mean of four surface heights (also 0.5 m raster) can be seen as a proxy for vegetation height and is used as input for the proposed classification work-flow. Figure 2, right, visualizes the AHN surface elevations over the same area as shown in Figure 2, left. In this study AHN4 data was used, that was acquired in early spring 2020.

2.3 Class definition and Training data

The three pure classes considered here are Sand, Grass and Trees. For each of these classes training data was identified for 30 areas of 10 by 10 meters where these classes are found throughout the whole 3 years of the Superview-1 data availability. These 90 (3×30) areas were validated using the high spatial resolution aerial photos.

3. METHODOLOGY

The classification methods considered are nearest centroid, random forest and neural network classification. These methods vary from easy to understand, but less flexible, to state-of-the-art models that are more difficult to tune. These classification methods are used to produce several vegetation assessment products. Their products are also used to compare and validate the models.

3.1 Nearest centroid

The first model is the simplest of the models considered, as it only involves one distance per class for each pixel to be classified, (Gou et al., 2012). The first step is to find the centroid, or mean, of the features of the training data of each target class, so there are as many centroids as there are classes. The construction of these centroids is a simple arithmetic mean, which computational effort scales linearly with the amount of training points (Schütze et al., 2008).

To get a classification for a pixel p, the Euclidean distance of the features of pixel p to each centroid $c_i, i = 1, 2, 3$ is calculated in feature space. The centroid at smallest distance has the highest probability, and is assumed to correspond to the class the pixel belongs to. In addition, a probability $P(C_i, p)$ for class membership of pixel p to each class C_i is obtained by Eqn. 1

$$P(C_i, p) = 1 - \frac{d_i}{d_1 + d_2 + d_3}, \qquad i = 1, \ldots, 3 \qquad (1)$$

with:

d_i = distance $d(p, c_i)$ to centroid c_i of class i

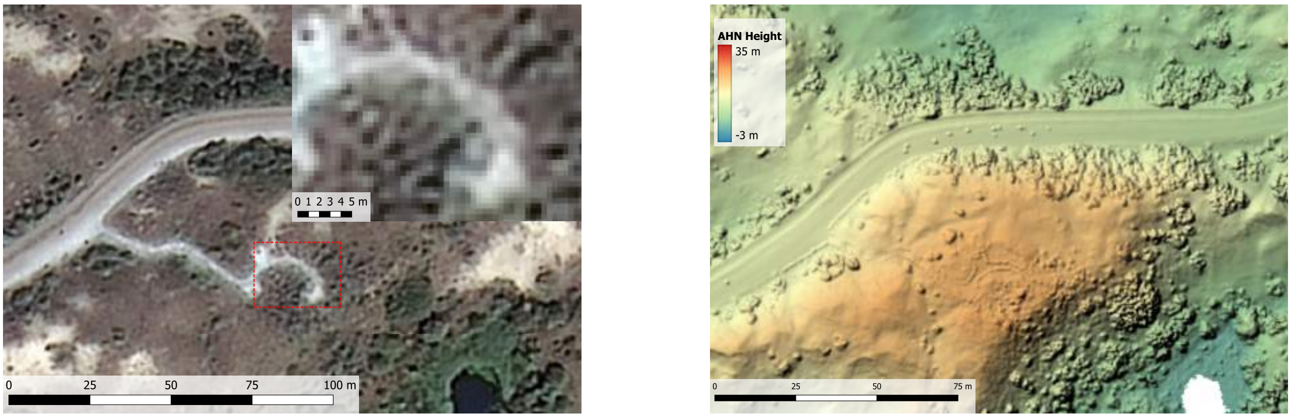

Figure 2. **Left:** Superview true color satellite image with zoom-in of the red rectangle at pixel level. **Right:** AHN4 airborne LIDAR surface elevations of the same area.

3.2 Random forest

The random forest model (Breiman, 2001) is a method that combines multiple decision trees into an ensemble. One such decision tree makes binary choices in feature space to get the best splits. The tree leafs correspond to the target classes. The best split is identified by minimizing the Gini impurity, which is a measure to quantify the quality of a split, (Breiman et al., 1984). Correlation between different decision trees is decreased by: (i) using only part of the training data for building one tree, and, (ii) by also using only part of the features for building one tree.

To classify an unseen pixel, its features are run through all, 100 decision trees of the random forest. The pixel is assigned to the class which most trees vote for. In addition, the percentage of trees voting for a class is interpreted as the probability that the pixel belongs to that class.

3.3 Neural network

A Neural network is a type of machine learning model, based on the concept of how neurons in brains learn. It is one of the most advanced classification methods available. These models consist of at least three layers, the input layer, one or more hidden layers and one output layer. Each layer consists of a number of neurons (or nodes) which are connected to all or some of the neurons from the layer before and after. These connections all have a modifiable weight (or strength). These values will be estimated during the training of the model by minimizing a suitable loss function in an iterative way, (Wang, 2003, Bishop and Nasrabadi, 2006).

The number of input nodes is equal to the number of data sources that are put into the model, which is five in our case, RGBI + ΔH. The part with the hidden layers is where the model does the work, and the number of layers, the number of nodes in each layer and an activation function need to be determined. Our model consists of one hidden layer of 14 neurons. The output of a node is determined by the non-linear activation function, that scales the weighted sum of each input connection. There are several possibilities for this activation function, including the sigmoid, the arc tangent and hyperbolic tangents functions. In our case, the number of outputs will be equal to the number of classes, and a softmax activation function is used, which is considered best for categorical outputs. The output layer consist of three 'class' neurons, one for Trees, Sand and Grass.

To train the neural network, the weights of all the connections between the nodes have to be optimized. This requires a large training data set, which the model will use to find relations between the input layers and the output class in the training data. The progress is evaluated by a loss function that quantifies the difference between the neural network output and the training data. The loss function used is categorical cross-entropy loss. The final output will produce a value at each output node that is interpreted as the probability that a previously unseen pixel belongs to that class.

4. RESULTS

Using all three classification methods, a land cover classification and a probability map were created for each of the RGBI Superview-1 images in Table 2. Input in all epochs was the latest Superview-1 RGBI image, at 1 m resolution, plus AHN4 derived vegetation height ΔH. Note that ΔH is available from a single acquisition only, and thus does not change over time. Known locations with water and buildings were masked out using a static mask based on the national topographic map. This multi-epoch classifications also results in a land cover timeline.

Here, only the classification results based on the Superview data of 2021-09-07 will be shown in combination with the ΔH height. This Superview data has the best quality from the recent imagery, while the AHN4 data acquisition time of 2020 is not too far away.

In Section 4.1 the Neural Network classification results will be presented, followed by single pixel probabilities in Section 4.2. Class variations through time will be shown in Section 4.3, while class transitions will be showcased in Section 4.4. Some results of Nearest Centroid and Random Forest will be discussed in Chapter 5.

4.1 Neural network classification result

The classification result of the neural network, implemented using TensorFlow (Abadi et al., 2015), is shown in Figure 3. Here, the left image shows the final class labels, while the right image also visualises the class probabilities. The overall map looks as expected, with sandy patches closer to the sea at the west and

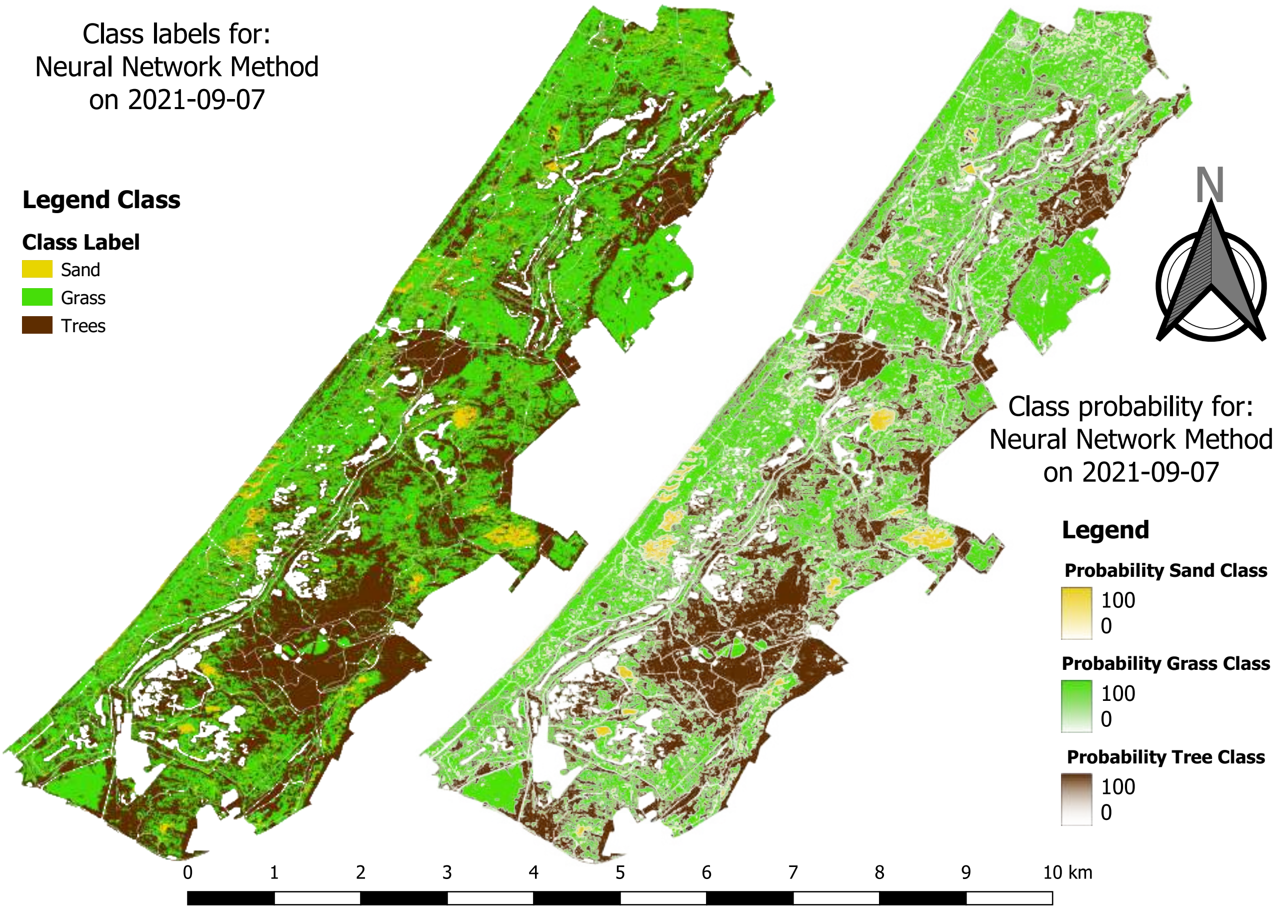

Figure 3. **Left:** Class labels as classified by the Neural Network method. **Right:** Probability of classes, grey pixel would mean low probability for every class.

more trees inland, i.e. the east part of the area. The confusion matrix in Table 3 also shows that the testing data shows very good agreement with the training data, with accuracies between 97% and 100% for all classes. This agreement is expected to be lower near class transitions, due to mixed pixel effects, where one pixel contains vegetation from several classes, but also because of gradual vegetation transitions in the field, for example sand, mixed with small patches of vegetation.

Neural Network	Sand	Grass	Trees	**User acc.**
Sand	460	0	0	100%
Grass	0	528	12	97%
Trees	0	4	596	99%
Producers acc.	100%	99%	97%	99%

Table 3. Confusion matrix for the neural network model classification on 2021-09-07. Here, 'acc.' stands for accuracy

4.2 Probability triangle plot

As indicated in Section 3.3, per pixel probabilities of each of the three classes, Sand, Trees, and Grass, are also saved. The resulting probabilities for the Neural Network classification are shown in Figure 4. In this scatter plot each classified pixel, p, is positioned according to each three probability values, p_1 for Trees, p_2 for Sand, and p_3 for Grass. At the vertices of the triangle, pixels are located with 100% probability for one class. In general, a pixel, p, is positioned in the probability triangle at position t_p according to its barycentric coordinates, (Möbius,

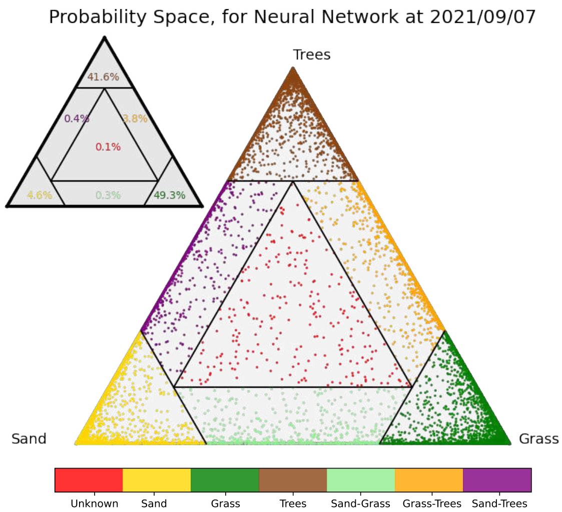

Figure 4. Scatter plot of pixel probabilities as output by the Neural Network method. The small triangle at the top left shows the percentage of pixels for each of the seven sub-polygons of the big triangle. The 4-gons along the edges of the big triangle are interpreted as mixed classes like 'Grass-Trees'.

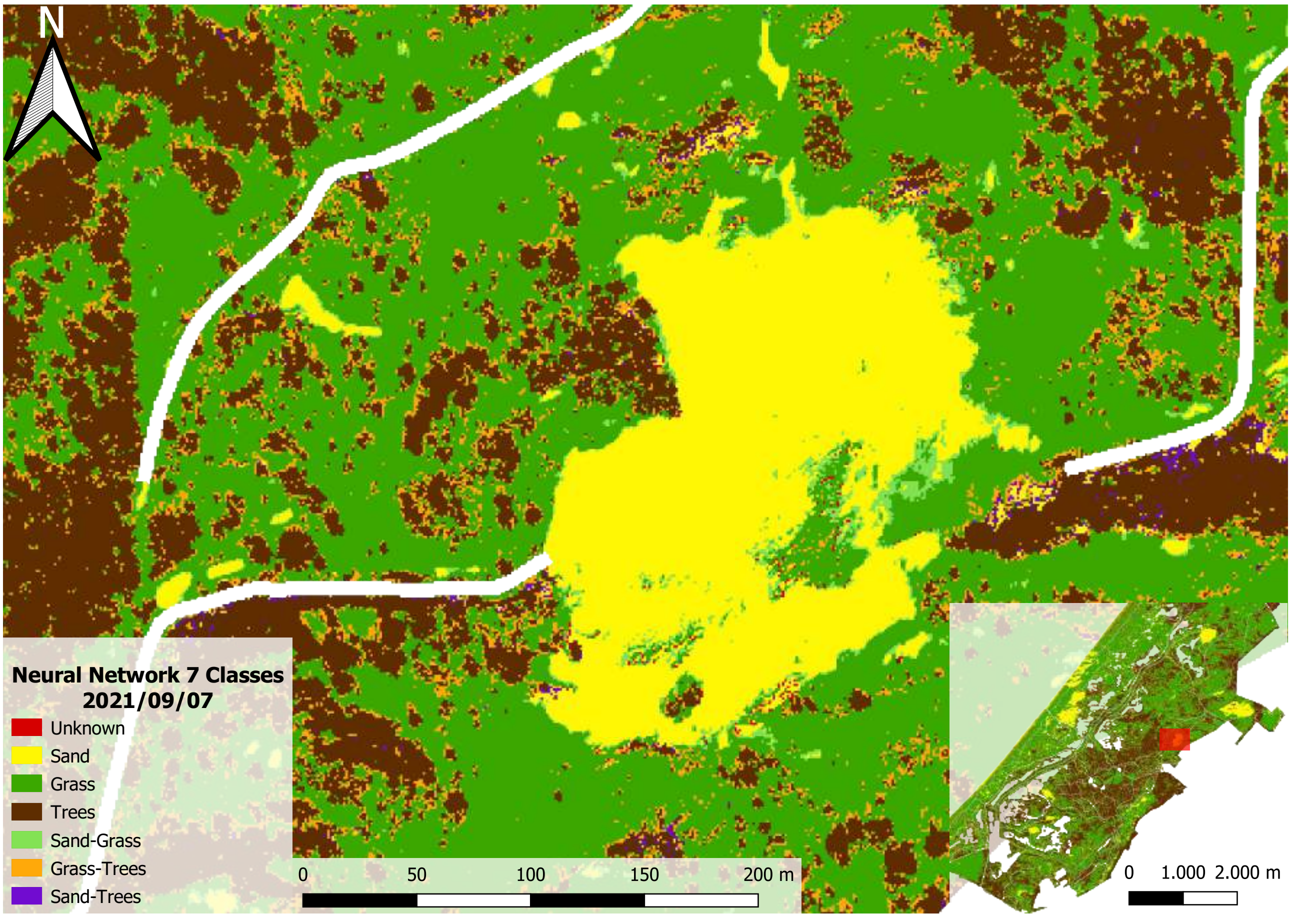

Figure 5. Map showing location of pure and fuzzy class pixels, as obtained by the Neural Network classification. The fuzzy sub-classes are indeed located on the expected transition zones.

1827), as indicated in Eqn. 2.

$$t_p = p_1 \cdot T + p_2 \cdot S + p_3 \cdot G \tag{2}$$

$$1 = p_1 + p_2 + p_3 \tag{3}$$

In Eqn. 2, the symbols T, S and G refer to the positions in Figure 4 of the vertices corresponding to pure Trees, Sand, and Grass respectively, while Eqn. 3 expresses that total probability equals 1.

The probability plot in Figure 4 is subdivided into seven polygons. The three triangles in the corners contain the pixels with a dominant probability of at least 70%, while the 4-gons aligned with the edges have a low probability, (<15%), for the opposite class. These 4-gons could also be seen as fuzzy transition classes, like 'Sand-Grass'. The triangle in the middle contains pixels with no dominant probability, (not above 85%), for any of the three classes.

The small gray triangle at the top left of Figure 4 shows which percentages of pixels fall within each pure class or transition class. Most pixels (both over 40%) are classified as Grass or Trees, while only 4.6% of the pixels is classified as sand. The transition class Grass-Trees also receives 3.8% of the pixels. The unknown class in the middle contains only 0.1% of the pixels.

The location of some of the pixels belonging to these fuzzy transition classes is shown in Figure 5. This figure contains a zoom-in of the neural network classification results. Indeed, as expected, transition pixels, like 'Grass-Sand' are found on the borders where Grass and Sand meet. This indicates that the transition classes actually show transitions and not pixels that are classified wrongly.

4.3 Class distribution through time

The timeline in Figure 6 shows the percentage of pixels per pure and fuzzy class over the area as a whole for each of the 11 Neural Network classification results of the Superview-1 images enriched with AHN4 height, as indicated in Table 2.

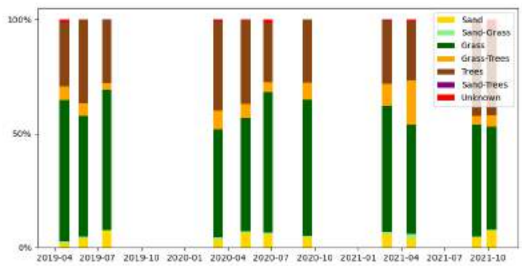

Figure 6. Percentage of pixels per pure and fuzzy class for each of the 11 Neural Network classifications of individual Superview-1 images enriched by AHN4 height.

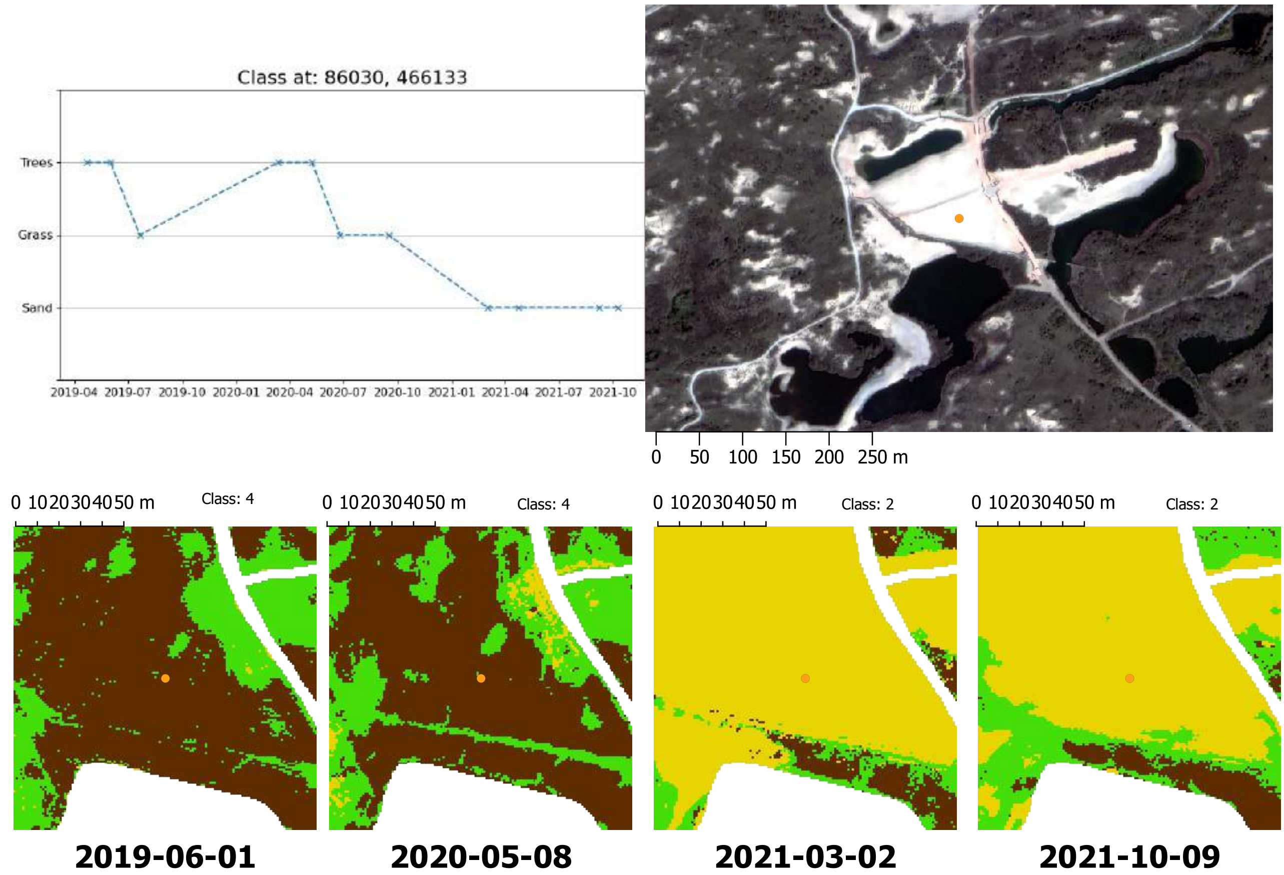

Figure 7. Classification results at and around a fixed point though time. The top right shows a recent areal photo with a query point indicated by a yellow dot. The graph at the top left shows the class predictions by the neural network for that location for each of the 11 Superview-1 images enriched with height. The pixel starts as Tree, changes to Grass and ends as Sand. The bottom row shows four classification results for different times, clearly demonstrating the transition from Trees to Sand for this case study area.

The results show some consistency over time, with Grass always as the biggest class, followed by Trees. The class Sand is comparable in size to the fuzzy class Grass-Trees, while the other two fuzzy classes Sand-Grass and Sand-Trees as well as the Unknown class only have small percentages of pixels. Further analysis is required to understand the variation in percentages in Figure 6, which could be caused by seasonal influences for example, as vegetation is more abundant in summer, while, in addition, there are different seasonal patterns for different types of vegetation.

4.4 Case Study Berkheide

Larger and sudden changes are easily picked up by the Neural Network classification results. This is demonstrated in Figure 7, which shows class transitions at a known construction site. In this case a whole area in the Berkheide area has been cleared of bushes and trees to create a new region for water infiltration. This project started at the end of October 2020, (Spierenburg, 2020), as can be seen in the timeline on the top left of Figure 7.

5. DISCUSSION

In this discussion we cover three topics, first classification scope in Section 5.1, followed by a discussion on the results of the other two methods in Section 5.2. This chapter is concluded by a discussion on the probabilities obtained by these two methods in Section 5.3.

5.1 Classification scope

These classification methods were specially designed for the vegetation in coastal area's. Given the success of the classification, it is expected that more classes could be extracted from the data, e.g. the Trees and Grass classes could be further specified towards individual species. Extra classes would however require additional training data, and would increase the computational efforts of training the system. Water could be made into a class, as water presence is varying throughout years and seasons. However, including a water class or other classes might worsen the accuracy of the vegetation classification which is our priority.

5.2 Nearest Centroid and Random Forest classifications

The other classification methods tested were nearest centroid and Random Forest classification. The nearest centroid results show the limitations of this method. While it is fast, requiring 40 seconds per time step, the accuracies were lowest at 95% and by relying only on the distance to the closest class centroid, it is apparently difficult to distinguish grass from trees, due to the proximity of their centroids. As a result, much more grass is found than with the other methods.

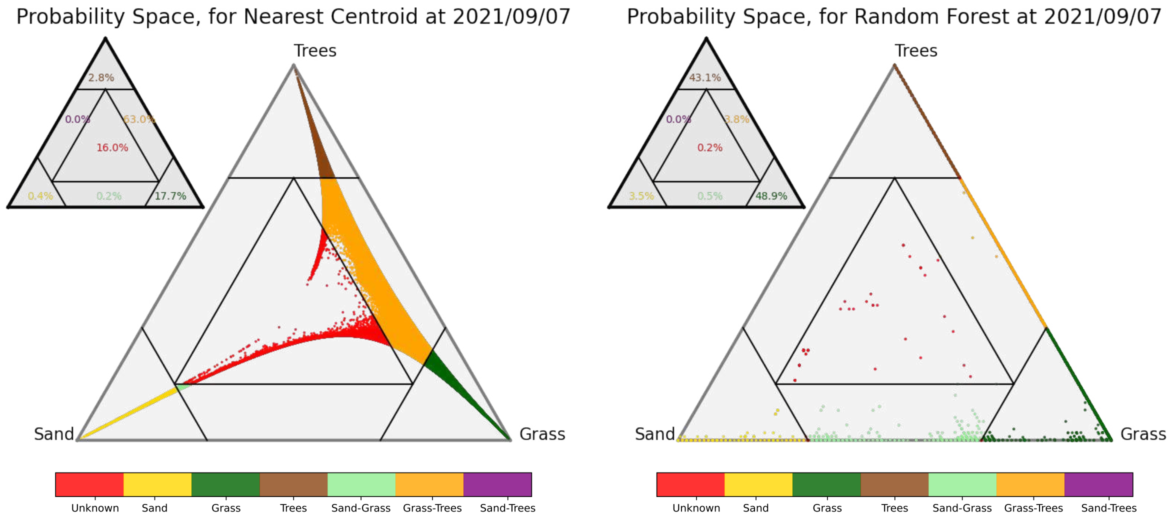

Figure 8. Scatter plot of pixel probabilities as output by the Nearest Centroid method, left, and the Random Forest method, right. In both cases, the percentage of pixels for each of the seven sub-polygons is given in the small triangles at the top left of each scatter plot.

The Random Forest method produced results which are similar to the neural network results, with similar high (>97%) accuracy. However the Neural Network model is better suited for working with large datasets and is computationally faster than the Random Forest classification. The Neural Network needs about 100 seconds per time step, while the Random forest needs about 210 seconds. The major difference is in the class transitions, where Random Forest has low bushes included in the tree class, while the neural network classifies these as part of the grass class. A main advantage of the Random Forest method over the neural network is the ability to analyze exactly how the method makes its decision.

5.3 Probabilities, Nearest Centroid and Random Forest

The scatter plots of the pixel probabilities are interesting as they are very different for the three methods considered. In addition to the Neural Network scatter plot, Figure 4, scatter plots of pixel probabilities are given in Figure 8 for the Nearest Centroid results, left, and for the Random Forest results, right.

The Nearest Centroid scatter plot in Figure 8, left, shows a smooth pattern connecting all corners, but leaving large parts of the probability space systematically blank. Reason for these empty parts is that the probabilities are based on distances in feature space: if a feature coincides with a class centroid, it will be in one of the vertices of the probability triangle; if, on the other hand, it does not coincide, it will have non-zero distance to all three centroids and therefore stay away from the triangle edges. The scatter plot is slightly shifted towards the Grass-Trees side, however all pixels have positive probability for each pure class. 16% of the pixels is located in the middle unknown part while a large amount of 63% belongs to the Grass-Trees class, again, because the class centroids of the training samples of Grass and Trees are close in feature space. For this method, probabilities of one are reached only once the feature vector of a pixel coincides with the centroid of a training sample.

A contrasting pattern is observed for the Random Forest probabilities. Here the probabilities form a linear or discrete pattern caused by the fact that probability is always a number of trees. So if none of the trees vote for a class, the pixel will fall on the outer edge of the triangle. In this case there are slightly more points in the mixed classes than in case of the Neural Network example.

Overall, the probability scatter plots helps understanding the properties of different classification methods, while mixed probabilities may correspond to transitions between classes in practice. Note that none of these methods were specifically designed or trained to produce fuzzy results, here we merely grasped the opportunity to analyze outcomes in this direction.

6. CONCLUSION

This study shows that dunal vegetation monitoring is possible from readily available remote sensing sources. We showed that using a combination of satellite spectral, and aerial LiDAR data the vegetation can be classified in three major classes: trees, grass, and sand, as well as their transition zones. The satellite spectral data used has sub-meter spatial resolution, comparable to the dedicated surveys currently in use, and is therefore suitable for detailed vegetation assessment. Main benefit of using satellite observations over dedicated aerial surveys is, other than the reduced costs, a temporal resolution of months instead of years.

The new, higher, temporal resolution introduces new requirements on the acquisition of training data and ground truth data. To mitigate the need for new ground training points for every date, training should only be done on places with a homogeneous area where only a single class is found. Our experiments show that fuzzy classes can still be estimated, and that vegetation transitions are correctly identified.

ACKNOWLEDGEMENTS

The authors would like to thank Harrie van der Hagen (Dunea N.V.) for sharing his expert knowledge of the area, and current vegetation mapping strategy. Furthermore, the authors would like to acknowledge the Netherlands Space Office for providing the Superview data.

REFERENCES

Abadi, M., Agarwal, A., Barham, P., Brevdo, E., Chen, Z., Citro, C., Corrado, G. S., Davis, A., Dean, J., Devin, M., Ghemawat, S., Goodfellow, I., Harp, A., Irving, G., Isard, M., Jia, Y., Jozefowicz, R., Kaiser, L., Kudlur, M., Levenberg, J., Mané, D., Monga, R., Moore, S., Murray, D., Olah, C., Schuster, M., Shlens, J., Steiner, B., Sutskever, I., Talwar, K., Tucker, P., Vanhoucke, V., Vasudevan, V., Viégas, F., Vinyals, O., Warden, P., Wattenberg, M., Wicke, M., Yu, Y., Zheng, X., 2015. TensorFlow: Large-scale machine learning on heterogeneous systems. Software available from tensorflow.org.

Ackerly, D. D., Cornwell, W. K., Weiss, S. B., Flint, L. E., Flint, A. L., 2015. A geographic mosaic of climate change impacts on terrestrial vegetation: which areas are most at risk? *PloS one*, 10(6), e0130629.

Assendorp, D. et al., 2010. Classification of Patterns and Process in Small-scale Dynamic Ecosystems: With Cases in the Dutch Coastal Dunes. PhD thesis, Universiteit van Amsterdam.

Bishop, C. M., Nasrabadi, N. M., 2006. *Pattern recognition and machine learning*. Springer.

Breiman, L., 2001. Random forests. *Machine learning*, 45(1), 5–32.

Breiman, L., Friedman, J., Stone, C. J., Olshen, R. A., 1984. *Classification and regression trees*. CRC press.

De Lange, R., van Til, M., Dury, S., 2004. The use of hyperspectral data in coastal zone vegetation monitoring. *EARSeL eProceedings*, 3(2), 143–153.

Feilhauer, H., Zlinszky, A., Kania, A., Foody, G. M., Doktor, D., Lausch, A., Schmidtlein, S., 2021. Let your maps be fuzzy!—Class probabilities and floristic gradients as alternatives to crisp mapping for remote sensing of vegetation. *Remote Sensing in Ecology and Conservation*, 7(2), 292–305.

Gou, J., Yi, Z., Du, L., Xiong, T., 2012. A local mean-based k-nearest centroid neighbor classifier. *The Computer Journal*, 55(9), 1058–1071.

Kukunda, C. B., Duque-Lazo, J., González-Ferreiro, E., Thaden, H., Kleinn, C., 2018. Ensemble classification of individual Pinus crowns from multispectral satellite imagery and airborne LiDAR. *International Journal of Applied Earth Observation and Geoinformation*, 65, 12–23.

Liu, Y.-K., Ma, L.-L. et al., 2020. On-orbit radiometric calibration of the optical sensors on-board SuperView-1 satellite using three independent methods. *Optics Express*, 28(8), 11085–11105.

Möbius, A. F., 1827. *Der barycentrische Calcul*. Barth, Leipzig.

Mozgovoy, D., Hnatushenko, V. V., Vasyliev, V. V., 2018. Automated recognition of vegetation and water bodies on the territory of megacities in satellite images of visible and IR bands. *ISPRS Annals of Photogrammetry, Remote Sensing and Spatial Information Sciences*, IV-3, 167-172.

Mücher, C. A., Roupioz, L., Kramer, H., Bogers, M., Jongman, R. H., Lucas, R. M., Kosmidou, V., Petrou, Z., Manakos, I., Padoa-Schioppa, E. et al., 2015. Synergy of airborne LiDAR and Worldview-2 satellite imagery for land cover and habitat mapping: A BIO_SOS-EODHaM case study for the Netherlands. *International Journal of Applied Earth Observation and Geoinformation*, 37, 48–55.

Schütze, H., Manning, C. D., Raghavan, P., 2008. *Introduction to information retrieval*. Cambridge University Press, Cambridge.

Soilán Rodríguez, M., Lindenbergh, R., Riveiro Rodríguez, B., Sánchez Rodríguez, A., 2019. Pointnet for the automatic classification of aerial point clouds. *ISPRS Annals of Photogrammetry, Remote Sensing and Spatial Information Sciences*, IV-2/W5, 445—452.

Spierenburg, P., 2020. Eerste project Programma Berkheide van start. https://www.dunea.nl/zakelijk/nieuwsbrieven/nieuwsbrief-2020-10/eerste-project-programma-berkheide-van-start.

Sundseth, K., Creed, P., 2008. *Natura 2000: protecting Europe's biodiversity*. European Commission Luxembourg.

Tapia, R., Stein, A., Bijker, W., 2005. Optimization of sampling schemes for vegetation mapping using fuzzy classification. *Remote Sensing of Environment*, 99(4), 425–433.

Van Natijne, A., Lindenbergh, R., Hanssen, R., 2018. Massive linking of PS-InSAR deformations to a national airborne laser point cloud. *International Archives Photogrammetry Remote Sensing and Spatial Information Sciences*, 42(2), 1137–1144.

Wang, S.-C., 2003. *Interdisciplinary Computing in Java Programming*. Springer, Boston, MA, chapter Artificial neural network, 81–100.